

Infrared divergences in light-front QED and coherent state basis

Jai D. More^{*} and Anuradha Misra[†]

Department of Physics, University of Mumbai, Santa Cruz (East), Mumbai 400098, India

(Received 26 June 2012; published 26 September 2012)

We present a next-to-leading-order calculation of electron mass renormalization in light-front quantum electrodynamics using old-fashioned time-ordered perturbation theory. We show that the true infrared divergences in δm^2 get canceled up to $O(e^4)$ if one uses the coherent state basis instead of the Fock basis to calculate the transition matrix elements.

DOI: [10.1103/PhysRevD.86.065037](https://doi.org/10.1103/PhysRevD.86.065037)

PACS numbers: 11.10.Ef, 12.20.Ds, 12.38.Bx

I. INTRODUCTION

It is well known that in quantum electrodynamics (QED), the infrared (IR) divergences get canceled in suitably defined cross sections by virtue of the famous Bloch-Nordsieck theorem [1]. According to this theorem, the divergences in virtual processes get canceled when the contribution of real photon emission is added. It is to be noted that this cancellation takes place at the level of cross sections and not at the level of amplitudes. The divergences at the amplitude level arise due to inappropriate choices of initial and final states. In Lehmann-Symanzik-Zimmermann formulation, the dynamics of incoming and outgoing particles in a scattering event is described by the free Hamiltonian, and therefore, the initial and final states used to calculate the transition matrix elements are taken to be Fock states. However, in an actual experiment, due to the finite size of the detector, the charged particle can be accompanied by any number of photons. The Bloch-Nordsieck mechanism takes into account all states with any number of soft photons below experimental resolution, thus leading to cancellation of the divergences. The issue of cancellation of IR divergences at the amplitude level was addressed by Chung [2], who showed that the divergences in matrix elements are eliminated to all orders in perturbation theory if one chooses the initial and final states to be charged particles with a suitable superposition of an infinite number of photons. Kulish and Faddeev (KF) [3] defined the asymptotic states by means of an asymptotic Hamiltonian. They were the first to show that in QED, the asymptotic Hamiltonian does not coincide with the free Hamiltonian. Kulish and Faddeev constructed the asymptotic Hamiltonian V_{as} for QED, thus modifying the asymptotic condition to introduce a new space of asymptotic states given by

$$|n; \pm\rangle = \Omega_{\pm}^A |n\rangle, \quad (1)$$

where Ω_{\pm}^A is the asymptotic evolution operator and $|n\rangle$ is the Fock state. Ω_{\pm}^A is defined by

^{*}more.physics@gmail.com

[†]misra@physics.mu.ac.in

$$\Omega_{\pm}^A = T \exp \left[-i \int_{\mp}^0 V_{as}(t) dt \right]. \quad (2)$$

KF further modified the definition of the S matrix and showed that it is free of IR divergences. In a nutshell, the method of asymptotic dynamics proposed by KF replaces the free Hamiltonian with an asymptotic Hamiltonian which takes into account the long-range interaction between incoming and outgoing states and can be used to construct a set of coherent states as the asymptotic states. The transition matrix elements formed by using these states are then free of infrared divergences.

The KF method was used by Nelson and Butler [4–6] to generate a set of asymptotic states in the asymptotic region of perturbative quantum chromodynamics. The asymptotic states constructed were shown to lead to the cancellation of IR divergences in certain matrix elements in the lowest order in perturbative quantum chromodynamics. Greco *et al.* [7] constructed a coherent state approach for non-Abelian gauge theories and showed that matrix elements between coherent states of definite color are finite and factorized in the fixed-angle regime. The KF method was also applied to QCD by Dahmein and Steiner [8], who showed that the leading logarithmic behavior of the mass shell form factor can be derived from the asymptotic quark gluon part of the QCD Hamiltonian.

Relevance of coherent state formalism in light-front field theory (LFFT) was first discussed by Harindranath and Vary [9], who showed that a coherent state may be a valid vacuum in LFFT. Later, it was shown [10] in the context of the light-front Schwinger model that the physical vacuum is a gauge-invariant superposition of coherent states of dynamical gauge field zero mode.

A coherent state formalism for light-front quantum electrodynamics (LFQED) was developed by one of us in Ref. [11], henceforth referred to as I , as a possible method to deal with the *true* IR divergences of LFFT. These true IR divergences are the bona fide divergences of equal-time field theory and appear when both k^+ and \mathbf{k}_{\perp} approach zero. In addition to these, there are additional IR divergences in LFFT called the *spurious* IR divergences, as they are just a manifestation of ultraviolet divergences of

equal-time theory. It was shown in I that the true IR divergences in one-loop vertex correction are eliminated when the transition matrix element is calculated between the coherent states in place of Fock states. Subsequently, it was proposed [12] to use the coherent state basis constructed in I for the calculation of Hamiltonian matrix elements in the discrete light cone quantization method of bound state calculation as a possible way to avoid the vanishing energy denominators and the resulting true IR divergences. The method was applied to obtain the light-cone Schrödinger equation for positronium using the coherent state basis, and to demonstrate the absence of Coulomb singularity therein. The method of asymptotic dynamics has also been applied to light-front quantum chromodynamics (LFQCD) [13] to obtain a set of coherent states, and it has been shown to lead to the cancellation of IR divergences appearing due to vanishing energy denominators (which are actually the true IR divergences) in qqg vertex correction at the one-loop level.

The KF method leads to the cancellation of IR divergences in QED to all orders. However, it is well known that the Bloch-Nordsieck theorem does not hold in QCD, and therefore, in this case one does not expect to construct an all-order proof of cancellation of IR divergences along the lines of the KF method. Basically, the non-cancellation of IR divergences in QCD stems from the fact that asymptotic states here are bound states of quarks and antiquarks, and therefore the asymptotic Hamiltonian to be used in the KF method should contain the confining potential, and is not just the asymptotic Hamiltonian of QCD. An “improved” method of asymptotic dynamics was introduced by McMullan *et al.* [14–16], which also takes into account the separation of particles. The improved method has also been discussed in the context of LFQED and LFQCD [17].

In this work, we calculate fermion self-energy in LFQED up to $O(e^4)$. We extend the analysis of I to include the instantaneous interaction also in the construction of the asymptotic Hamiltonian and the resulting coherent state basis. We show that the true IR divergences in electron mass renormalization are canceled up to $O(e^4)$ if one uses the coherent state basis for evaluating the transition matrix elements.

Conventionally, LF quantization is performed in the light-front gauge, $A^+ = 0$, due to its many advantages when applied to non-Abelian theory [18]—specifically due to the absence of ghost fields. In this work on QED, we have also used the light-front gauge. There has been some discussion addressing the question of gauge independence of LFQED calculations in the literature [19]. In a recent work, the gauge independence of nonperturbative calculations of the electron’s anomalous magnetic moment has been verified [20]. However, in this work, we have not addressed the issue of gauge dependence of our results, as we plan to do this in a future work.

The cancellation of IR divergences in covariant QED has been established to all orders in both the amplitude as well as the cross-section approach. Various authors [21–24] have addressed the issue of equivalence of covariant and light-front formalism of field theory, and therefore it may be considered unnecessary to address the cancellation of IR divergence in LFFT. However, the divergence structure of LFFT is different from that of covariant formalism, and there are issues present that still need to be addressed [25]. In particular, it is important to differentiate between true and spurious IR divergences. As discussed in Refs. [11–13, 17], a coherent state approach in LFFT is interesting due to the following reason: LFFT being based on a Hamiltonian approach, a coherent state method in LFFT may be useful from the point of view of extracting information about the artificial confining potential which is needed in LF bound state calculations [26]. It is well known that IR divergences do not cancel in QCD, and the reason within the coherent state formalism is that the asymptotic states are not the asymptotic states of QCD but are bound states of quarks and antiquarks. In other words, if we use the appropriate Hamiltonian of bound states as the asymptotic Hamiltonian and develop a coherent state approach based on it, then this approach would lead to the cancellation of IR divergences in QCD as well. It will be worthwhile to understand this connection between the cancellation/noncancellation of IR divergences and the form of the asymptotic Hamiltonian. The hope is that by understanding the structure of IR divergences, we may be able to get some insight into the form of artificial confining potential mentioned in Ref. [26], which can then be used to perform the bound state calculations.

The plan of the paper is as follows: In Sec. II, we present the Hamiltonian of LFQED and calculate the $O(e^2)$ electron mass renormalization using light-cone time-ordered perturbation theory in the standard Fock basis. We demonstrate the appearance of true IR divergences in the form of vanishing light-cone energy denominators. In Sec. III, we obtain the form of coherent states using the method of asymptotic dynamics. In Sec. IV, we calculate δm^2 in the lowest order using the coherent state basis and show that the extra contributions due to emission and absorption of soft photons indeed cancel the IR divergences in δm^2 . In Sec. V, we calculate δm^2 up to $O(e^4)$ in the Fock basis and identify the IR divergences in it. In Sec. VI, we perform the same calculation in the coherent state basis and show the cancellation of IR divergences in this basis. Section VII contains a summary and discussion of our results. In Appendix A, we set the notations and conventions and give some useful relations. Appendix B contains some useful properties of coherent states. Appendixes C and D contain the details of the calculation of the transition matrix element in the Fock basis and the coherent state basis, respectively.

II. PRELIMINARIES

A. Light-front QED Hamiltonian

The light-front QED Hamiltonian in the light-front gauge ($A^+ = 0$) expressed in terms of independent degrees of freedom is given by Refs. [27,28]:

$$P^- = H \equiv H_0 + V_1 + V_2 + V_3, \quad (3)$$

where

$$H_0 = \int d^2\mathbf{x}_\perp dx^- \left\{ \frac{i}{2} \bar{\xi} \gamma^- \vec{\partial}_- \xi + \frac{1}{2} (F_{12})^2 - \frac{1}{2} a_+ \partial_- \partial_k a_k \right\}, \quad (4)$$

is the free Hamiltonian,

$$V_1 = e \int d^2\mathbf{x}_\perp dx^- \bar{\xi} \gamma^\mu \xi a_\mu, \quad (5)$$

is the standard $O(e)$ three-point interaction,

$$V_2 = -\frac{i}{4} e^2 \int d^2\mathbf{x}_\perp dx^- dy^- \epsilon(x^- - y^-) \times (\bar{\xi} a_k \gamma^k)(x) \gamma^+ (a_j \gamma^j \xi)(y). \quad (6)$$

is an $O(e^2)$ nonlocal effective four-point interaction corresponding to an instantaneous fermion exchange, and

$$V_3 = -\frac{e^2}{4} \int d^2\mathbf{x}_\perp dx^- dy^- (\bar{\xi} \gamma^+ \xi)(x) |x^- - y^-| (\bar{\xi} \gamma^+ \xi)(y), \quad (7)$$

is an $O(e^2)$ nonlocal effective four-point interaction corresponding to an instantaneous photon exchange. V_2 and V_3 are drawn as four-point interactions, and a hash mark is drawn on the line representing the instantaneous particle. $\xi(x)$ and $a_\mu(x)$ can be expanded in terms of creation and annihilation operators as

$$\begin{aligned} \xi(x) &= \int \frac{d^2\mathbf{p}_\perp}{(2\pi)^{3/2}} \\ &\times \int \frac{dp^+}{\sqrt{2p^+}} \sum_{s=\pm\frac{1}{2}} [u(p, s) e^{-i(p^+ x^- - \mathbf{p}_\perp x_\perp)} b(p, s, x^+) \\ &+ v(p, s) e^{i(p^+ x^- - \mathbf{p}_\perp x_\perp)} d^\dagger(p, s, x^+)], \end{aligned} \quad (8)$$

$$\begin{aligned} a_\mu(x) &= \int \frac{d^2\mathbf{q}_\perp}{(2\pi)^{3/2}} \int \frac{dq^+}{\sqrt{2q^+}} \sum_{\lambda=1,2} \epsilon_\mu^\lambda(q) \\ &\times [e^{-i(q^+ x^- - \mathbf{q}_\perp x_\perp)} a(q, \lambda, x^+) \\ &+ e^{i(q^+ x^- - \mathbf{q}_\perp x_\perp)} a^\dagger(q, \lambda, x^+)], \end{aligned} \quad (9)$$

where

$$\begin{aligned} \{b(p, s), b^\dagger(p', s')\} &= \delta(p^+ - p'^+) \delta^2(\mathbf{p}_\perp - \mathbf{p}'_\perp) \delta_{ss'} \\ &= \{d(p, s), d^\dagger(p', s')\}, \end{aligned} \quad (10)$$

$$[a(q, \lambda), a^\dagger(q', \lambda')] = \delta(q^+ - q'^+) \delta^2(\mathbf{q}_\perp - \mathbf{q}'_\perp) \delta_{\lambda\lambda'}. \quad (11)$$

These relations hold at equal light-front time x^+ . In terms of these momentum-space operators, the free Hamiltonian has the form

$$\begin{aligned} H_0 &= \int d^2\mathbf{p}_\perp dp^+ \left[\frac{\mathbf{p}_\perp^2 + m^2}{2p^+} \sum_{s=\pm\frac{1}{2}} (b^\dagger(p, s) b(p, s) \right. \\ &\left. + d^\dagger(p, s) d(p, s)) + \frac{\mathbf{p}_\perp^2}{2p^+} \sum_{\lambda=1,2} a^\dagger(p, s) a(p, s) \right]. \end{aligned} \quad (12)$$

Similarly, V_1 has the form

$$\begin{aligned} V_1 &= e \int d^2\mathbf{x}_\perp dx^- \int [dp][d\bar{p}][dk] \\ &\times \sum_{s,s',\lambda} [e^{i\bar{p}\cdot x} \bar{u}(\bar{p}, s') b^\dagger(\bar{p}, s') + e^{-i\bar{p}\cdot x} \bar{v}(\bar{p}, s') d(\bar{p}, s')] \\ &\times \gamma^\mu [e^{-ip\cdot x} u(p, s) b(p, s) + e^{ip\cdot x} v(p, s) d^\dagger(p, s)] \\ &\times \epsilon_\mu^\lambda(k) [e^{-ik\cdot x} a(k, \lambda) + e^{ik\cdot x} a^\dagger(k, \lambda)], \end{aligned} \quad (13)$$

where

$$\int [dp] \equiv \int_{-\infty}^{\infty} \frac{d^2\mathbf{p}_\perp}{(2\pi)^2} \int_0^\infty \frac{dp^+}{\sqrt{2p^+}}. \quad (14)$$

V_2 and V_3 are given by the following expressions:

$$\begin{aligned} V_2 &= -\frac{ie^2}{4} \int d^2\mathbf{x}_\perp dx^- dy^- dl [dp][d\bar{p}][dk][d\bar{k}] \\ &\times \sum_{s,s',\lambda,\lambda'} \left[-\frac{i}{\pi l} \right] e^{il(x^- - y^-)} [e^{ip\cdot x} \bar{u}(p, s) b^\dagger(p, s) \\ &+ e^{-ip\cdot x} \bar{v}(p, s) d(p, s)] \not{\epsilon}^\lambda(k) [e^{-ik\cdot x} a(k, \lambda) \\ &+ e^{ik\cdot x} a^\dagger(k, \lambda)] \gamma^+ \not{\epsilon}^{\lambda'}(\bar{k}) [e^{-i\bar{p}\cdot y} u(\bar{p}, s') b(\bar{p}, s') \\ &+ e^{i\bar{p}\cdot y} v(\bar{p}, s') d^\dagger(\bar{p}, s')] [e^{-i\bar{k}\cdot y} a(\bar{k}, \lambda') \\ &+ e^{i\bar{k}\cdot y} a^\dagger(\bar{k}, \lambda')], \end{aligned} \quad (15)$$

$$\begin{aligned} V_3 &= \frac{e^2}{4} \int d^2\mathbf{x}_\perp dx^- dy^- dl [dp][d\bar{p}][dk][d\bar{k}] \\ &\times \sum_{s,s',\sigma,\sigma'} \frac{e^{il(x^- - y^-)}}{\pi l^2} [e^{i\bar{p}\cdot x} \bar{u}(\bar{p}, s') b^\dagger(\bar{p}, s') \\ &+ e^{-i\bar{p}\cdot x} \bar{v}(\bar{p}, s') d(\bar{p}, s')] \gamma^+ [e^{-ip\cdot x} u(p, s) b(p, s) \\ &+ e^{ip\cdot x} v(p, s) d^\dagger(p, s)] [e^{i\bar{k}\cdot y} \bar{u}(\bar{k}, \sigma') b^\dagger(\bar{k}, \sigma') \\ &+ e^{-i\bar{k}\cdot y} \bar{v}(\bar{k}, \sigma') d(\bar{k}, \sigma')] \gamma^+ [e^{-ik\cdot y} u(k, \sigma) b(k, \sigma) \\ &+ e^{ik\cdot y} v(k, \sigma) d^\dagger(k, \sigma)], \end{aligned} \quad (16)$$

where $y = (x^+, y^-, \mathbf{x}_\perp)$.

B. Electron mass renormalization in light-front QED

In light-front time-ordered perturbation theory, the transition matrix is given by the perturbative expansion

$$T = V + V \frac{1}{p^- - H_0} V + \dots \quad (17)$$

The electron mass shift is obtained by calculating T_{pp} , which is the matrix element of the above series between the initial and the final electron states $|p, s\rangle$ and $|p, \sigma\rangle$, and it is given by Ref. [28] as

$$\delta m^2 = p^+ \sum_s T_{pp}. \quad (18)$$

Note that only $\sigma = s$ contributes, as the fermion self-energy is diagonal in spin.

We expand T_{pp} in powers of e^2 as

$$T_{pp} = T^{(1)} + T^{(2)} + \dots \quad (19)$$

In general, $T^{(n)}$ gives the $O(e^{2n})$ contribution to electron self-energy correction. Here, the initial (or final) electron momentum is

$$p = \left[p^+, \frac{\mathbf{p}_\perp^2 + m^2}{2p^+}, \mathbf{p}_\perp \right]. \quad (20)$$

In particular, $O(e^2)$ correction is obtained from

$$\begin{aligned} T_{pp}^{(1)} &\equiv T^{(1)}(p, p) \\ &= \langle p, s | V_1 \frac{1}{p^- - H_0} V_1 | p, s \rangle + \langle p, s | V_2 | p, s \rangle. \end{aligned}$$

Note that

$$T_{pp}^{(1)} \equiv T^{(1)}(p, p) = T_{1a} + T_{1b}, \quad (21)$$

where T_{1a} and T_{1b} are $O(e^2)$ contributions from the standard three-point vertex and the four-point instantaneous vertex, and are represented by the diagrams in Figs. 1(a) and 1(b), respectively. We are interested in the true IR divergences, which arise due to vanishing energy denominators in time-ordered perturbation theory [11]. It is obvious that T_{1b} cannot have such IR divergences, as there are no energy denominators involved, and hence this term is not required in our discussion. Neglecting T_{1b} , the $O(e^2)$ transition matrix element contributing to fermion self-energy reduces to

$$T_{1a}(p, p) = \langle p, s | V_1 \frac{1}{p^- - H_0} V_1 | p, s \rangle. \quad (22)$$

To calculate T_{1a} , we insert two complete sets of states so that the above equation becomes

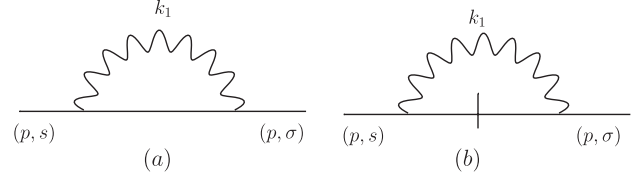


FIG. 1. Diagrams for $O(e^2)$ self-energy correction in the Fock basis corresponding to T_1 .

$$\begin{aligned} T_{1a}(p, p) &= \sum_{\text{spins}} \int \prod_{i=1}^2 d^3 p'_i d^3 k'_i \langle p, s | V_1 | p'_1, s'_1, k'_1, \lambda'_1 \rangle \\ &\quad \times \langle p'_1, s'_1, k'_1, \lambda'_1 | \frac{1}{p^- - H_0} | p'_2, s'_2, k'_2, \lambda'_2 \rangle \\ &\quad \times \langle p'_2, s'_2, k'_2, \lambda'_2 | V_1 | p, s \rangle. \end{aligned} \quad (23)$$

Substituting for V_1 from Eq. (13) and using Eqs. (18) and (A4), we obtain

$$\begin{aligned} \delta m_{1a}^2 &= \frac{e^2}{2(2\pi)^3} \int d^2 \mathbf{k}_{1\perp} \int \frac{dk_1^+}{k_1^+ p_1^+} \\ &\quad \times \frac{\text{Tr}[\not{\epsilon}^\lambda(k_1)(\not{p}_1 + m)\not{\epsilon}^\lambda(k_1)(\not{p} + m)]}{4(p^- - p_1^- - k_1^-)}, \end{aligned} \quad (24)$$

where $p_1 = p - k_1$. Calculating the trace, using Eq. (A9) for the energy denominator and taking the limit $k_1^+ \rightarrow 0$, $\mathbf{k}_{1\perp} \rightarrow 0$, we finally obtain

$$(\delta m_{1a}^2)^{\text{IR}} = -\frac{e^2}{(2\pi)^3} \int d^2 \mathbf{k}_{1\perp} \int \frac{dk_1^+}{k_1^+} \frac{(p \cdot \epsilon(k_1))^2}{(p \cdot k_1)}. \quad (25)$$

Note that the denominator vanishes as $k_1^+ \rightarrow 0$, $\mathbf{k}_{1\perp} \rightarrow 0$, leading to true IR divergences [11].

III. INFRARED DIVERGENCES AND THE COHERENT STATE BASIS

It was shown in *I* that the true IR divergences in one-loop vertex correction get canceled if one uses the coherent state basis in LFQED. We will prove the same result for electron mass renormalization in Sec. IV. For that purpose, we will now obtain the form of coherent states in light-front formalism by the method used in Ref. [3] for equal time theory. In *I*, only the three-point vertex was used to obtain the asymptotic Hamiltonian and the corresponding coherent state basis. We extend the formalism developed in *I* by obtaining the asymptotic limit of four-point instantaneous interaction also.

The light-front time dependence of the interaction Hamiltonian is given by

$$H_I(x^+) = V_1(x^+) + V_2(x^+) + V_3(x^+),$$

where [11]

$$V_1(x^+) = e \sum_{i=1}^4 \int d\nu_i^{(1)} [e^{-i\nu_i^{(1)} x^+} \tilde{h}_i^{(1)}(\nu_i^{(1)}) + e^{i\nu_i^{(1)} x^+} \tilde{h}_i^{(1)\dagger}(\nu_i^{(1)})], \quad (26)$$

and $\tilde{h}_i^{(1)}(\nu_i^{(1)})$ are three-point QED interaction vertices:

$$\tilde{h}_1^{(1)} = \sum_{s,s',\lambda} b^\dagger(\bar{p}, s') b(p, s) a(k, \lambda) \bar{u}(\bar{p}, s') \gamma^\mu u(p, s) \epsilon_\mu^\lambda, \quad (27)$$

$$\tilde{h}_2^{(1)} = \sum_{s,s',\lambda} b^\dagger(\bar{p}, s') d^\dagger(p, s) a(k, \lambda) \bar{u}(\bar{p}, s') \gamma^\mu v(p, s) \epsilon_\mu^\lambda, \quad (28)$$

$$\tilde{h}_3^{(1)} = \sum_{s,s',\lambda} d(\bar{p}, s') b(p, s) a(k, \lambda) \bar{v}(\bar{p}, s') \gamma^\mu u(p, s) \epsilon_\mu^\lambda, \quad (29)$$

$$\tilde{h}_4^{(1)} = \sum_{s,s',\lambda} d^\dagger(\bar{p}, s') d(p, s) a(k, \lambda) \bar{v}(\bar{p}, s') \gamma^\mu v(p, s) \epsilon_\mu^\lambda, \quad (30)$$

and $\nu_i^{(1)}$ is the light-front energy transferred at the vertex $\tilde{h}_i^{(1)}$. For example,

$$\nu_1^{(1)} = p^- + k^- - \bar{p}^- = \frac{p \cdot k}{p^+ + k^+}, \quad (31)$$

is the energy transfer at the $ee\gamma$ vertex. The integration measure is given by

$$\int d\nu^{(1)} = \frac{1}{(2\pi)^{3/2}} \int \frac{[dp][dk]}{\sqrt{2\bar{p}^+}}, \quad (32)$$

with \bar{p}^+ and $\bar{\mathbf{p}}_\perp$ being fixed at each vertex by momentum conservation.

At asymptotic limits, nonzero contributions to $V_1(x^+)$ come from regions where $\nu_i^{(1)} \rightarrow 0$. It is easy to see that $\nu_2^{(1)}$ and $\nu_3^{(1)}$ are always nonzero, and therefore \tilde{h}_2 and \tilde{h}_3 do not appear in the asymptotic Hamiltonian. Thus, the three-point asymptotic Hamiltonian is defined by the following expression [11]:

$$V_{1as}(x^+) = e \sum_{i=1,4} \int d\nu_i^{(1)} \Theta_\Delta(k) [e^{-i\nu_i^{(1)} x^+} \tilde{h}_i^{(1)}(\nu_i^{(1)}) + e^{i\nu_i^{(1)} x^+} \tilde{h}_i^{(1)\dagger}(\nu_i^{(1)})], \quad (33)$$

where $\Theta_\Delta(k)$ is a function which takes the value 1 in the asymptotic region and is 0 elsewhere.

As shown in *I*, for V_1 we can define the asymptotic region to consist of all points in the phase space for which

$$\frac{p \cdot k}{p^+} < \Delta E, \quad (34)$$

where ΔE is an energy cutoff which may be chosen to be the experimental resolution. For simplicity, we shall choose a frame $\mathbf{p}_\perp = 0$. In this frame, the above condition reduces to

$$\frac{p^+ \mathbf{k}_\perp^2}{2k^+} + \frac{m^2 k^+}{2p^+} < \Delta, \quad (35)$$

where $\Delta = p^+ \Delta E$.

Thus, for all the points satisfying Eq. (35), $\nu_1^{(1)}$ and $\nu_4^{(1)}$ can be approximated by zero. This implies that in this region, the asymptotic Hamiltonian is different from the free Hamiltonian. For the present purpose, i.e., in order to eliminate the true IR divergences, we find it sufficient to choose a subregion of the above mentioned region as the asymptotic region. We define this subregion to be consisting of all points (k^+, \mathbf{k}_\perp) satisfying

$$\mathbf{k}_\perp^2 < \frac{k^+ \Delta}{p^+}, \quad (36)$$

$$k^+ < \frac{p^+ \Delta}{m^2}. \quad (37)$$

This choice of the asymptotic region leads to the asymptotic interaction Hamiltonian defined by Eq. (33) with

$$\Theta_\Delta(k) = \theta\left(\frac{k^+ \Delta}{p^+} - \mathbf{k}_\perp^2\right) \theta\left(\frac{p^+ \Delta}{m^2} - k^+\right). \quad (38)$$

The contribution to the asymptotic Hamiltonian from the four-point instantaneous interaction can be obtained by taking the $|x^+| \rightarrow \infty$ limit in $V_2(x^+)$. $V_2(x^+)$ is given by

$$V_2(x^+) = e^2 \sum_{i=1}^8 \int d\nu_i^{(2)} [e^{-i\nu_i^{(2)} x^+} \tilde{h}_i^{(2)}(\nu_i^{(2)}) + e^{i\nu_i^{(2)} x^+} \tilde{h}_i^{(2)\dagger}(\nu_i^{(2)})] \frac{1}{2(\pm p^+ \pm k_1^+)}, \quad (39)$$

where $\tilde{h}_i^{(2)}(\nu_i^{(2)})$ are four-point instantaneous fermion exchange vertices. For example,

$$\begin{aligned} \tilde{h}_1^{(2)} &= \sum_{s,s',\lambda_1,\lambda_2} b^\dagger(\bar{p}, s') b(p, s) a(k_1, \lambda_1) a(k_2, \lambda_2) \bar{u}(\bar{p}, s') \\ &\times \gamma^\mu \gamma^+ \gamma^\nu u(p, s) \epsilon_\mu^{\lambda_1}(k_1) \epsilon_\nu^{\lambda_2}(k_2). \end{aligned}$$

One can write the remaining seven terms in a similar manner. $\nu_i^{(2)}$ is the light-front energy transferred at the vertex $\tilde{h}_i^{(2)}$. For example, in Eq. (39),

$$\begin{aligned} \nu_2^{(2)} &= p^- - k_1^- + k_2^- - \bar{p}^- \\ &= -\frac{p \cdot k_1 - p \cdot k_2 + k_1 \cdot k_2}{p^+ - k_1^+ + k_2^+}, \end{aligned} \quad (40)$$

and the integration measure is

$$\int d\nu^{(2)} = \frac{1}{(2\pi)^{3/2}} \int \frac{[dp][dk_1][dk_2]}{\sqrt{2\bar{p}^+}}. \quad (41)$$

At asymptotic limits, nonzero contributions to $V_2(x^+)$ come from regions where $\nu_i^{(2)} \rightarrow 0$. It can be shown easily that $\nu_2^{(2)}$ and $\nu_8^{(2)}$ vanish when $k_1^+ = k_2^+$ and $\mathbf{k}_{1\perp} = \mathbf{k}_{2\perp}$, while the rest of the six $\nu_i^{(2)}$'s are always nonzero. Thus, the asymptotic Hamiltonian for V_2 is defined by the following expression:

$$V_{2as}(x^+) = e^2 \sum_{i=2,8} \int d\nu_i^{(2)} \delta^3(k_1 - k_2) [e^{-i\nu_i^{(2)}x^+} \tilde{h}_i^{(2)}(\nu_i^{(2)}) + e^{i\nu_i^{(2)}x^+} \tilde{h}_i^{(2)\dagger}(\nu_i^{(2)})] \frac{1}{2(p^+ - k_1^+)}. \quad (42)$$

Similarly, $V_{3as}(x^+)$ is obtained by taking the limit $|x^+| \rightarrow \infty$ in $V_3(x^+)$, where

$$V_3(x^+) = e^2 \sum_{i=1}^8 \int d\nu_i^{(3)} [e^{-i\nu_i^{(3)}x^+} \tilde{h}_i^{(3)}(\nu_i^{(3)}) + e^{i\nu_i^{(3)}x^+} \tilde{h}_i^{(3)\dagger}(\nu_i^{(3)})] \frac{1}{2(\pm p^+ \pm \bar{p}^+)^2}. \quad (43)$$

Here, $\tilde{h}_i^{(3)}(\nu_i^{(3)})$ are four-point instantaneous photon exchange vertices. One can easily verify that $\nu_i^{(3)}$'s are always nonzero for all i . Hence, $V_3(x^+)$ is zero in the asymptotic limit and does not contribute to the asymptotic Hamiltonian.

The asymptotic states can be defined in the usual manner by

$$|n: coh\rangle = \Omega_{\pm}^A |n\rangle, \quad (44)$$

where $|n\rangle$ is a Fock state, and Ω_{\pm}^A are the asymptotic Möller operators defined by

$$\Omega_{\pm}^A = T \exp \left[-i \int_{\mp}^0 [V_{1as}(x^+) + V_{2as}(x^+)] dx^+ \right]. \quad (45)$$

Carrying out the standard procedure [3] of substituting $k^+ = 0$, $\mathbf{k}_{\perp} = 0$ in all the slowly varying functions of k , and carrying out the x^+ integration, we arrive at the following expression for the asymptotic states:

$$\begin{aligned} \Omega_{\pm}^A |n: p_i\rangle = & \exp \left[-e \int dp^+ d^2\mathbf{p}_{\perp} \int \sum_{\lambda=1,2} \frac{d^2\mathbf{k}_{\perp}}{(2\pi)^{3/2}} \int \frac{dk^+}{\sqrt{2k^+}} [f(k, \lambda: p) a^{\dagger}(k, \lambda) - f^*(k, \lambda: p) a(k, \lambda)] \right. \\ & + e^2 \int dp^+ d^2\mathbf{p}_{\perp} \int \sum_{\lambda_1=1,2} \frac{d^2\mathbf{k}_{1\perp}}{(2\pi)^{3/2}} \int \frac{dk_1^+}{\sqrt{2k_1^+}} \int \sum_{\lambda_2=1,2} \frac{d^2\mathbf{k}_{2\perp}}{(2\pi)^{3/2}} \\ & \times \left. \int \frac{dk_2^+}{\sqrt{2k_2^+}} [g_1(k_1, k_2, \lambda_1, \lambda_2: p) a^{\dagger}(k_2, \lambda_2) a(k_1, \lambda_1) - g_2(k_1, k_2, \lambda_1, \lambda_2: p) a(k_2, \lambda_2) a^{\dagger}(k_1, \lambda_1)] \rho(p) \right] |n: p_i\rangle, \end{aligned} \quad (46)$$

where

$$f(k, \lambda: p) = \frac{p_{\mu} \epsilon_{\lambda}^{\mu}(k)}{p \cdot k} \theta \left(\frac{k^+ \Delta}{p^+} - \mathbf{k}_{\perp}^2 \right) \theta \left(\frac{p^+ \Delta}{m^2} - k^+ \right), \quad (47)$$

$$f(k, \lambda: p) = f^*(k, \lambda: p), \quad (48)$$

$$g_1(k_1, k_2, \lambda_1, \lambda_2: p) = -\frac{4p^+}{p \cdot k_1 - p \cdot k_2 + k_1 \cdot k_2} \delta^3(k_1 - k_2), \quad g_2(k_1, k_2, \lambda_1, \lambda_2: p) = \frac{4p^+}{p \cdot k_1 - p \cdot k_2 - k_1 \cdot k_2} \delta^3(k_1 - k_2), \quad (49)$$

$$\rho(p) = \sum_n [b_n^{\dagger}(p) b_n(p) - d_n^{\dagger}(p) d_n(p)]. \quad (50)$$

Applying the operator $\rho(p)$ on the Fock state, we finally obtain

$$\begin{aligned}
\Omega_{\pm}^A |n: p_i\rangle = & \exp \left[-e \int \sum_{\lambda=1,2} \frac{d^2 \mathbf{k}_{\perp}}{(2\pi)^{3/2}} \int \frac{dk^+}{\sqrt{2k^+}} [f(k, \lambda, p) a^\dagger(k, \lambda) - f^*(k, \lambda, p) a(k, \lambda)] \right. \\
& + e^2 \int \sum_{\lambda_1=1,2} \frac{d^2 \mathbf{k}_{1\perp}}{(2\pi)^{3/2}} \int \frac{dk_1^+}{\sqrt{2k_1^+}} \int \sum_{\lambda_2=1,2} \frac{d^2 \mathbf{k}_{2\perp}}{(2\pi)^{3/2}} \int \frac{dk_2^+}{\sqrt{2k_2^+}} [g_1(k_1, k_2, \lambda_1, \lambda_2: p) a^\dagger(k_2, \lambda_2) a(k_1, \lambda_1) \\
& \left. - g_2(k_1, k_2, \lambda_1, \lambda_2: p) a(k_2, \lambda_2) a^\dagger(k_1, \lambda_1)] \right] |n: p_i\rangle.
\end{aligned} \tag{51}$$

In particular, the one-fermion coherent state is given by

$$\begin{aligned}
|p, \sigma: f(p)\rangle = & \exp \left[-e \int \sum_{\lambda=1,2} \frac{d^2 \mathbf{k}_{\perp}}{(2\pi)^{3/2}} \int \frac{dk^+}{\sqrt{2k^+}} [f(k, \lambda: p) a^\dagger(k, \lambda) - f^*(k, \lambda: p) a(k, \lambda)] \right. \\
& + e^2 \int \sum_{\lambda_1=1,2} \frac{d^2 \mathbf{k}_{1\perp}}{(2\pi)^{3/2}} \int \frac{dk_1^+}{\sqrt{2k_1^+}} \int \sum_{\lambda_2=1,2} \frac{d^2 \mathbf{k}_{2\perp}}{(2\pi)^{3/2}} \int \frac{dk_2^+}{\sqrt{2k_2^+}} [g_1(k_1, k_2, \lambda_1, \lambda_2: p) a^\dagger(k_2, \lambda_2) a(k_1, \lambda_1) \\
& \left. - g_2(k_1, k_2, \lambda_1, \lambda_2: p) a(k_2, \lambda_2) a^\dagger(k_1, \lambda_1)] \right] |p, \sigma\rangle.
\end{aligned} \tag{52}$$

Some useful properties of these coherent states are listed in Appendix B.

IV. ELECTRON MASS RENORMALIZATION UP TO $O(e^2)$ IN THE COHERENT STATE BASIS

In the coherent state basis, $O(e^2)$ self-energy contribution is given by $T^{(1)} + T'^{(1)}$, where $T^{(1)}$ is defined in Eq. (21) and $T'^{(1)}$ arises from the $O(e^2)$ term in

$$T'(p, p) = \langle p, s: f(p) | V_1 | p, s: f(p) \rangle, \tag{53}$$

with $|p, s: f(p)\rangle$ being the coherent state given by Eq. (52). The contribution of the $O(e)$ term in $f(p)$ leads to additional diagrams shown in Figs. 2(a) and 2(b), and is denoted by $T'_{2a} + T'_{2b}$. Here a dotted line represents the soft photon in the coherent state. The diagrams in Fig. 2 correspond to the emission (absorption) of a soft photon by the incoming (outgoing) fermion, but since the emitted (absorbed) photon is soft, the two-particle state containing it is indistinguishable from a single-fermion state. Substituting for V_1 from Eq. (13), we obtain

$$\begin{aligned}
T'(p, p) = & \frac{e}{(2\pi)^{3/2}} \int [d\bar{p}_1] [dp_1] [dk_1] \frac{\bar{u}(\bar{p}_1, s'_1) \not{\epsilon}^\lambda(k_1) u(p_1, s_1)}{\sqrt{2\bar{p}_1^+} \sqrt{2p_1^+} \sqrt{2k_1^+}} \\
& \times [\langle p, s: f(p) | b^\dagger(\bar{p}_1, s'_1) b(p_1, s_1) a(k_1, \lambda) | p, s: f(p) \rangle \delta^3(\bar{p}_1 - p_1 - k_1) \\
& + \langle p, s: f(p) | b^\dagger(\bar{p}_1, s'_1) b(p_1, s_1) a^\dagger(k_1, \lambda) | p, s: f(p) \rangle \delta^3(\bar{p}_1 - p_1 + k_1)].
\end{aligned} \tag{54}$$

Using coherent state properties [Eqs. (B1) and (B3) from Appendix B] in Eq. (54), we obtain

$$\begin{aligned}
T'(p, p) = & \frac{e^2}{(2\pi)^3} \int \frac{d^2 \mathbf{k}_{1\perp}}{2p^+} \int \frac{dk_1^+}{2k_1^+} \bar{u}(\bar{p}, s') \not{\epsilon}^\lambda(k_1) u(p, s) f(k_1, \lambda: p).
\end{aligned} \tag{55}$$

Using Eqs. (18) and (A4) and calculating the trace, we obtain

$$(\delta m^2)' = \frac{e^2}{(2\pi)^3} \int d^2 \mathbf{k}_{1\perp} \int \frac{dk_1^+}{k_1^+} \frac{(p \cdot \epsilon(k_1))^2 \Theta_\Delta(k_1)}{p \cdot k_1}, \tag{56}$$

where the prime indicates the correction due to additional terms in the coherent state basis. The energy denominator

in Eq. (56) vanishes in the limit $k_1^+ \rightarrow 0$, $\mathbf{k}_{1\perp} \rightarrow 0$, thus leading to IR divergences. However, when adding Eqs. (25) and (56), these true IR divergences get canceled, and the $O(e^2)$ electron mass correction is IR divergence free.

V. ELECTRON MASS RENORMALIZATION UP TO $O(e^4)$ IN THE FOCK BASIS

We will now calculate the $O(e^4)$ electron mass correction in the Fock basis. The transition matrix element for $O(e^4)$ correction to self-energy is given by

$$T^{(2)} = T_3 + T_4 + T_5 + T_6 + T_7, \tag{57}$$

where

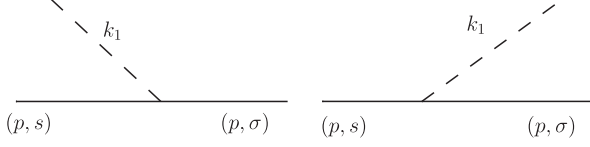


FIG. 2. Additional diagrams in the coherent state basis for $O(e^2)$ self-energy correction corresponding to T_2 .

$$T_3 = \langle p, s | V_1 \frac{1}{p^- - H_0} V_1 \frac{1}{p^- - H_0} V_1 \frac{1}{p^- - H_0} V_1 | p, s \rangle, \quad (58)$$

$$T_4 = \langle p, s | V_1 \frac{1}{p^- - H_0} V_1 \frac{1}{p^- - H_0} V_2 | p, s \rangle, \quad (59)$$

$$T_5 = \langle p, s | V_1 \frac{1}{p^- - H_0} V_2 \frac{1}{p^- - H_0} V_1 | p, s \rangle, \quad (60)$$

$$T_6 = \langle p, s | V_2 \frac{1}{p^- - H_0} V_1 \frac{1}{p^- - H_0} V_1 | p, s \rangle, \quad (61)$$

$$T_7 = \langle p, s | V_2 \frac{1}{p^- - H_0} V_2 | p, s \rangle. \quad (62)$$

These matrix elements correspond to Figs. 3–7 and can be evaluated in the standard manner by inserting the appropriate number of complete sets of intermediate states. We give the details of the calculation in Appendix C and present the results here.

T_3 is given by

$$T_3 \equiv T_3(p, p) = T_{3a} + T_{3b} + T_{3c}, \quad (63)$$

where T_{3a} , T_{3b} , and T_{3c} correspond to Figs. 3(a)–3(c) and are given by Eqs. (C1), (C4), and (C6) respectively. Using the expressions for the energy denominator in Eqs. (A9) and (A10) and using Eq. (18), we obtain

$$(\delta m^2)_{3a} = -\frac{e^4}{2(2\pi)^6} \int d^2\mathbf{k}_{1\perp} d^2\mathbf{k}_{2\perp} \int \frac{dk_1^+}{k_1^+} \frac{dk_2^+}{k_2^+} \frac{\text{Tr}[\not{\epsilon}^{\Lambda_1}(k_1)(\not{p}_1 + m)\not{\epsilon}^{\Lambda_2}(k_2)(\not{p}_2 + m)\not{\epsilon}^{\Lambda_2}(k_2)(\not{p}_1 + m)\not{\epsilon}^{\Lambda_1}(k_1)(\not{p} + m)]}{32(p \cdot k_1)^2[(p \cdot k_1) + (p \cdot k_2) - (k_1 \cdot k_2)]}, \quad (64)$$

$$(\delta m^2)_{3b} = -\frac{e^4}{2(2\pi)^6} \int d^2\mathbf{k}_{1\perp} d^2\mathbf{k}_{2\perp} \int \frac{dk_1^+}{k_1^+} \frac{dk_2^+}{k_2^+} \frac{\text{Tr}[\not{\epsilon}^{\Lambda_2}(k_2)(\not{p}_3 + m)\not{\epsilon}^{\Lambda_1}(k_1)(\not{p}_2 + m)\not{\epsilon}^{\Lambda_2}(k_2)(\not{p}_1 + m)\not{\epsilon}^{\Lambda_1}(k_1)(\not{p} + m)]}{32(p \cdot k_1)(p \cdot k_2)[(p \cdot k_1) + (p \cdot k_2) - (k_1 \cdot k_2)]}, \quad (65)$$

$$(\delta m^2)_{3c} = \frac{e^4}{2(2\pi)^6} \int d^2\mathbf{k}_{1\perp} d^2\mathbf{k}_{2\perp} \int \frac{dk_1^+}{k_1^+} \frac{dk_2^+}{p^+ k_2^+} \frac{\text{Tr}[\not{\epsilon}^{\Lambda_2}(k_2)(\not{p}_3 + m)\not{\epsilon}^{\Lambda_2}(k_2)(\not{p}_2' + m)\not{\epsilon}^{\Lambda_1}(k_1)(\not{p}_1 + m)\not{\epsilon}^{\Lambda_1}(k_1)(\not{p} + m)]}{32(p \cdot k_1)(p \cdot k_2)(p^- - p_2'^-)}, \quad (66)$$

where $p_2' = p$, and p_1 , p_2 , and p_3 have been defined in Eqs. (C2), (C3), and (C5), respectively.

Note that $(\delta m^2)_{3a}$, $(\delta m^2)_{3b}$, and $(\delta m^2)_{3c}$ can have IR divergences when

- (i) $p \cdot k_1 \rightarrow 0$, i.e., $k_1^+ \rightarrow 0$, $\mathbf{k}_{1\perp} \rightarrow 0$, but $p \cdot k_2 \neq 0$.
- (ii) $p \cdot k_2 \rightarrow 0$, i.e., $k_2^+ \rightarrow 0$, $\mathbf{k}_{2\perp} \rightarrow 0$, but $p \cdot k_1 \neq 0$.
- (iii) $p \cdot k_1 \rightarrow 0$ and $p \cdot k_2 \rightarrow 0$, i.e., $k_1^+ \rightarrow 0$, $\mathbf{k}_{1\perp} \rightarrow 0$, $k_2^+ \rightarrow 0$, $\mathbf{k}_{2\perp} \rightarrow 0$.

Now we will consider the contribution of Figs. 3(a)–3(c) in each of these limits.

Case I: In the limit $k_1^+ \rightarrow 0$, $\mathbf{k}_{1\perp} \rightarrow 0$ (but $p \cdot k_2 \not\rightarrow 0$), the contribution to T_3 from the diagrams in Figs. 3(a) and 3(b) is given by

$$[(\delta m^2)_{3a} + (\delta m^2)_{3b}]^I = -\frac{e^4}{(2\pi)^6} \int d^2\mathbf{k}_{1\perp} d^2\mathbf{k}_{2\perp} \int \frac{dk_1^+}{k_1^+} \frac{dk_2^+}{k_2^+} \frac{[2(p \cdot \epsilon(k_1))^2(p \cdot \epsilon(k_2))^2 - (p \cdot k_2)(p \cdot \epsilon(k_1))^2]}{4(p \cdot k_1)^2(p \cdot k_2)}, \quad (67)$$

and the contribution from Fig. 3(c) is given by

$$[(\delta m^2)_{3c}]^I = \frac{e^4}{(2\pi)^6} \int d^2\mathbf{k}_{1\perp} d^2\mathbf{k}_{2\perp} \int \frac{dk_1^+}{k_1^+} \frac{dk_2^+}{k_2^+} \frac{2(p \cdot \epsilon(k_1))^2(p \cdot \epsilon(k_2))^2 - (p \cdot k_2)(p \cdot \epsilon(k_1))^2}{8p^+} \times \left[\frac{p^+}{(p \cdot k_1)^2(p \cdot k_2)} + \frac{p_3^+}{(p \cdot k_1)(p \cdot k_2)^2} \right]. \quad (68)$$

Here we have used the Heitler method [29] illustrated in Appendix C to deal with the vanishing denominator $(p^- - p_2'^-)$.

Case II: In the limit $k_2^+ \rightarrow 0$, $\mathbf{k}_{2\perp} \rightarrow 0$ (but $p \cdot k_1 \not\rightarrow 0$), the contribution to T_3 from the diagrams in Figs. 3(a) and 3(b) is given by

$$[(\delta m^2)_{3a} + (\delta m^2)_{3b}]^{II} = -\frac{e^4}{(2\pi)^6} \int d^2\mathbf{k}_{1\perp} d^2\mathbf{k}_{2\perp} \int \frac{dk_1^+}{k_1^+} \frac{dk_2^+}{k_2^+} \frac{[2(p \cdot \epsilon(k_1))^2 (p \cdot \epsilon(k_2))^2 - (p \cdot k_1)(p \cdot \epsilon(k_2))^2]}{4(p \cdot k_1)(p \cdot k_2)^2}, \quad (69)$$

and the contribution from Fig. 3(c) is given by

$$[(\delta m^2)_{3c}]^{II} = \frac{e^4}{(2\pi)^6} \int d^2\mathbf{k}_{1\perp} d^2\mathbf{k}_{2\perp} \int \frac{dk_1^+}{k_1^+} \frac{dk_2^+}{k_2^+} \frac{2(p \cdot \epsilon(k_1))^2 (p \cdot \epsilon(k_2))^2 - (p \cdot k_1)(p \cdot \epsilon(k_2))^2}{8p^+} \times \left[\frac{p_1^+}{(p \cdot k_1)^2 (p \cdot k_2)} + \frac{p^+}{(p \cdot k_1)(p \cdot k_2)^2} \right]. \quad (70)$$

Case III: In the limit $k_1^+ \rightarrow 0$, $\mathbf{k}_{1\perp} \rightarrow 0$, $k_2^+ \rightarrow 0$, $\mathbf{k}_{2\perp} \rightarrow 0$, the contribution to T_3 from the diagrams in Figs. 3(a) and 3(b) is given by

$$[(\delta m^2)_{3a} + (\delta m^2)_{3b}]^{III} = -\frac{e^4}{(2\pi)^6} \int d^2\mathbf{k}_{1\perp} d^2\mathbf{k}_{2\perp} \int \frac{dk_1^+}{k_1^+} \frac{dk_2^+}{k_2^+} \frac{(p \cdot \epsilon(k_1))^2 (p \cdot \epsilon(k_2))^2}{2(p \cdot k_1)^2 (p \cdot k_2)}, \quad (71)$$

and the contribution from Fig. 3(c) is given by

$$[(\delta m^2)_{3c}]^{III} = \frac{e^4}{(2\pi)^6} \int d^2\mathbf{k}_{1\perp} d^2\mathbf{k}_{2\perp} \int \frac{dk_1^+}{k_1^+} \frac{dk_2^+}{k_2^+} \left[\frac{(p \cdot \epsilon(k_1))^2 (p \cdot \epsilon(k_2))^2}{4(p \cdot k_1)^2 (p \cdot k_2)} + \frac{(p \cdot \epsilon(k_1))^2 (p \cdot \epsilon(k_2))^2}{4(p \cdot k_1)(p \cdot k_2)^2} \right]. \quad (72)$$

The contributions to T_4 , T_5 , and T_6 come from the diagrams in Figs. 4–6, respectively. One can do similar calculations for the three cases by carefully taking the appropriate limits of the corresponding expressions. Below, we give contributions from these diagrams in each of the three limits.

Case I: In the limit $k_1^+ \rightarrow 0$, $\mathbf{k}_{1\perp} \rightarrow 0$ (but $p \cdot k_2 \not\rightarrow 0$), the contributions of the diagrams in Figs. 4(a), 5(a), 5(b), and 6(a) are given by

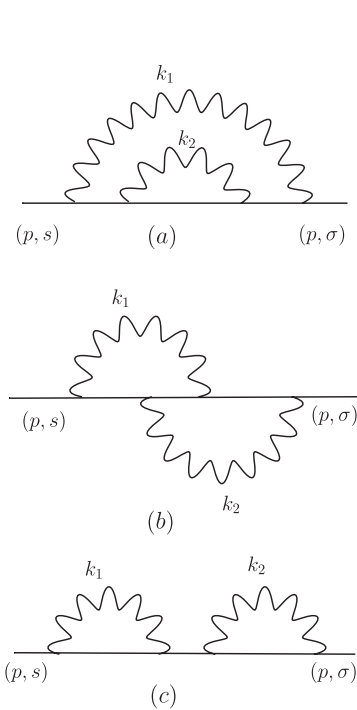


FIG. 3. Diagrams for $O(e^4)$ self-energy correction in the Fock basis corresponding to T_3 .

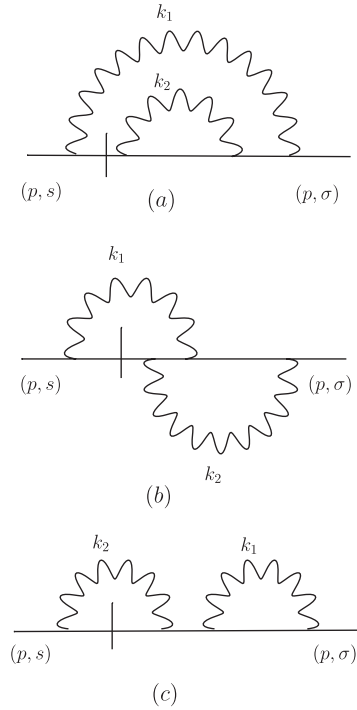


FIG. 4. Diagrams for $O(e^4)$ self-energy correction in the Fock basis corresponding to T_4 .

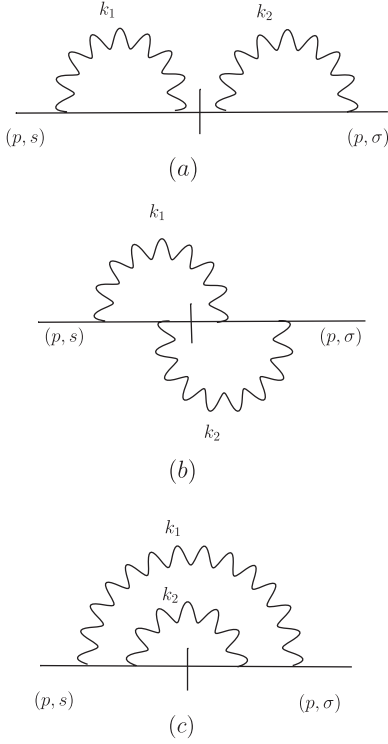


FIG. 5. Diagrams for $O(e^4)$ self-energy correction in the Fock basis corresponding to T_5 .

$$[(\delta m^2)_{4a}]^I = [(\delta m^2)_{6a}]^I = -\frac{e^4}{(2\pi)^6} \int d^2\mathbf{k}_{1\perp} d^2\mathbf{k}_{2\perp} \int \frac{dk_1^+}{k_1^+} \frac{dk_2^+}{k_2^+ p^+} \frac{[2p^+(p \cdot \epsilon(k_1))(p \cdot \epsilon(k_2))(\epsilon(k_1) \cdot \epsilon(k_2)) + k_2^+(p \cdot \epsilon(k_1))^2]}{8(p \cdot k_1)(p \cdot k_2)}, \quad (73)$$

$$[(\delta m^2)_{5a}]^I = -\frac{e^4}{(2\pi)^6} \int d^2\mathbf{k}_{1\perp} d^2\mathbf{k}_{2\perp} \int \frac{dk_1^+}{k_1^+} \frac{dk_2^+}{k_2^+ p^+} \frac{[2p^+(p \cdot \epsilon(k_1))(p \cdot \epsilon(k_2))(\epsilon(k_1) \cdot \epsilon(k_2)) + k_2^+(p \cdot \epsilon(k_1))^2]}{8(p \cdot k_1)(p \cdot k_2)}, \quad (74)$$

$$[(\delta m^2)_{5b}]^I = -\frac{e^4}{(2\pi)^6} \int d^2\mathbf{k}_{1\perp} d^2\mathbf{k}_{2\perp} \int \frac{dk_1^+}{k_1^+} \frac{dk_2^+}{k_2^+ p_3^+} \frac{[2p_3^+(p \cdot \epsilon(k_1))(p \cdot \epsilon(k_2))(\epsilon(k_1) \cdot \epsilon(k_2)) - k_2^+(p \cdot \epsilon(k_1))^2]}{8(p \cdot k_1)(p \cdot k_2)}. \quad (75)$$

The diagrams in Figs. 4(c), 5(c), and 6(c) have IR divergences only in limit I and lead to

$$[(\delta m^2)_{4c} + (\delta m^2)_{6c}]^I = -\frac{e^4}{(2\pi)^6} \int d^2\mathbf{k}_{1\perp} d^2\mathbf{k}_{2\perp} \int \frac{dk_1^+}{k_1^+} \frac{dk_2^+}{k_2^+} \frac{(p \cdot \epsilon(k_1))^2}{2(p \cdot k_1)^2}, \quad (76)$$

$$[(\delta m^2)_{5c}]^I = \frac{e^4}{(2\pi)^6} \int d^2\mathbf{k}_{1\perp} d^2\mathbf{k}_{2\perp} \int \frac{dk_1^+}{k_1^+} \frac{dk_2^+}{k_2^+} \frac{(p \cdot \epsilon(k_1))^2}{2(p \cdot k_1)^2}, \quad (77)$$

where again we have used the Heitler method for evaluating $T_{4c} + T_{6c}$. Figures 4(b) and 6(b) do not have IR divergences in this limit.

Case II: In the limit $k_2^+ \rightarrow 0$, $\mathbf{k}_{2\perp} \rightarrow 0$ (but $p \cdot k_1 \not\rightarrow 0$), the contributions of diagrams in Figs. 4(b), 5(a), 5(b), and 6(b) are given by the following expressions:

$$[(\delta m^2)_{4b}]^{II} = [(\delta m^2)_{6b}]^{II} = -\frac{e^4}{(2\pi)^6} \int d^2\mathbf{k}_{1\perp} d^2\mathbf{k}_{2\perp} \int \frac{dk_1^+}{k_1^+} \frac{dk_2^+}{k_2^+ p_1^+} \frac{[2p_1^+(p \cdot \epsilon(k_1))(p \cdot \epsilon(k_2))(\epsilon(k_1) \cdot \epsilon(k_2)) - k_1^+(p \cdot \epsilon(k_2))^2]}{8(p \cdot k_1)(p \cdot k_2)}, \quad (78)$$

$$[(\delta m^2)_{5a}]^{II} = -\frac{e^4}{(2\pi)^6} \int d^2\mathbf{k}_{1\perp} d^2\mathbf{k}_{2\perp} \int \frac{dk_1^+}{k_1^+} \frac{dk_2^+}{k_2^+ p_1^+} \frac{[2p_1^+(p \cdot \epsilon(k_1))(p \cdot \epsilon(k_2))(\epsilon(k_1) \cdot \epsilon(k_2)) + k_1^+(p \cdot \epsilon(k_2))^2]}{8(p \cdot k_1)(p \cdot k_2)}, \quad (79)$$

$$[(\delta m^2)_{5b}]^{II} = -\frac{e^4}{(2\pi)^6} \int d^2\mathbf{k}_{1\perp} d^2\mathbf{k}_{2\perp} \int \frac{dk_1^+}{k_1^+} \frac{dk_2^+}{k_2^+ p_1^+} \frac{[2p_1^+(p \cdot \epsilon(k_1))(p \cdot \epsilon(k_2))(\epsilon(k_1) \cdot \epsilon(k_2)) - k_1^+(p \cdot \epsilon(k_2))^2]}{8(p \cdot k_1)(p \cdot k_2)}. \quad (80)$$

Figures 4(a) and 6(a) do not have IR divergences in this limit. *Case III:* In the limit $k_1^+ \rightarrow 0$, $\mathbf{k}_{1\perp} \rightarrow 0$, $k_2^+ \rightarrow 0$, $\mathbf{k}_{2\perp} \rightarrow 0$, the sum of contributions corresponding to Figs. 4(a), 4(b), 6(a), and 6(b) is given by

$$[(\delta m^2)_{4a} + (\delta m^2)_{4b} + (\delta m^2)_{5a} + (\delta m^2)_{5b} + (\delta m^2)_{6a} + (\delta m^2)_{6b}]^{III} = -\frac{e^4}{(2\pi)^6} \int d^2\mathbf{k}_{1\perp} d^2\mathbf{k}_{2\perp} \int \frac{dk_1^+}{k_1^+} \frac{dk_2^+}{k_2^+} \frac{[(p \cdot \epsilon(k_1))(p \cdot \epsilon(k_2))(\epsilon(k_1) \cdot \epsilon(k_2))]}{(p \cdot k_1)(p \cdot k_2)}, \quad (81)$$

where we have used Eqs. (C22), (C27), (C30), and (C34). The last term, T_7 in Eq. (62), is IR convergent, as the four-point energy denominator involved here is nonzero, and hence T_7 is not needed for our discussion. One can notice that Eqs. (67)–(81) have true IR divergences, since the denominator vanishes as $k_1^+ \rightarrow 0$, $\mathbf{k}_{1\perp} \rightarrow 0$ and/or $k_2^+ \rightarrow 0$, $\mathbf{k}_{2\perp} \rightarrow 0$.

VI. ELECTRON MASS RENORMALIZATION IN THE COHERENT STATE BASIS UP TO $O(e^4)$

In this section, we will use the coherent state basis to calculate the $O(e^4)$ electron mass correction. We will show that the IR divergences in additional diagrams appearing due to the use of the coherent state basis exactly cancel the IR divergences arising due to the vanishing energy denominators calculated in Sec. V. In the coherent state basis, the $O(e^4)$ correction to self-energy is given by

$$T^{(2)} + T'_8 + T'_9 + T'_{10} + T'_{11},$$

where T'_8 is the $O(e^4)$ term in $\langle p, s: f(p) | V_1 \frac{1}{p-H_0} V_1 \frac{1}{p-H_0} V_1 | p, s: f(p) \rangle$ represented by Fig. 8, T'_9 is the $O(e^4)$ term in $\langle p, s: f(p) | V_1 \frac{1}{p-H_0} V_1 | p, s: f(p) \rangle$ represented by Fig. 9, T'_{10} is the $O(e^4)$ term in $\langle p, s: f(p) | V_1 \frac{1}{p-H_0} V_2 | p, s: f(p) \rangle + \langle p, s: f(p) | V_2 \frac{1}{p-H_0} V_1 | p, s: f(p) \rangle$ represented by Fig. 10, and T'_{11} is the $O(e^4)$ term in $\langle p, s: f(p) | V_2 | p, s: f(p) \rangle$ represented by Fig. 11. We present the details of calculation in Appendix D and give below only the result for $(\delta m^2)'$.

The contribution corresponding to Fig. 8 is given by

$$(\delta m^2)'_8 = (\delta m^2)'_{8a} + (\delta m^2)'_{8b} + (\delta m^2)'_{8c} + (\delta m^2)'_{8d} + (\delta m^2)'_{8e} + (\delta m^2)'_{8f}, \quad (82)$$

where $(\delta m^2)'_{8a}$ through $(\delta m^2)'_{8f}$ have been evaluated in Appendix D.

Figures 8(a) and 8(b) contribute

$$(\delta m^2)'_{8a} = \frac{e^4}{(2\pi)^6} \int d^2\mathbf{k}_{1\perp} d^2\mathbf{k}_{2\perp} \int \frac{dk_1^+}{k_1^+} \frac{dk_2^+}{k_2^+} \frac{[2(p \cdot \epsilon(k_1))^2(p \cdot \epsilon(k_2))^2 - (p \cdot k_2)(p \cdot \epsilon(k_1))^2]}{4(p \cdot k_1)^2[(p \cdot k_1) + (p \cdot k_2) - (k_1 \cdot k_2)]} \Theta_\Delta(k_1), \quad (83)$$

$$(\delta m^2)'_{8b} = \frac{e^4}{(2\pi)^6} \int d^2\mathbf{k}_{1\perp} d^2\mathbf{k}_{2\perp} \int \frac{dk_1^+}{k_1^+} \frac{dk_2^+}{k_2^+} \frac{[2(p \cdot \epsilon(k_1))^2(p \cdot \epsilon(k_2))^2]}{4(p \cdot k_1)(p \cdot k_2)[(p \cdot k_1) + (p \cdot k_2) - (k_1 \cdot k_2)]} \Theta_\Delta(k_1). \quad (84)$$

One can notice that for $(\delta m^2)'_{8a}$ and $(\delta m^2)'_{8b}$ we need not discuss limit II, as $p \cdot k_1$ is always small. Adding Eqs. (83) and (84) and taking the limit I, we obtain

$$[(\delta m^2)'_{8a} + (\delta m^2)'_{8b}]^I = \frac{e^4}{(2\pi)^6} \int d^2\mathbf{k}_{1\perp} d^2\mathbf{k}_{2\perp} \int \frac{dk_1^+}{k_1^+} \frac{dk_2^+}{k_2^+} \left[\frac{(p \cdot \epsilon(k_1))^2(p \cdot \epsilon(k_2))^2}{2(p \cdot k_1)^2(p \cdot k_2)} - \frac{(p \cdot \epsilon(k_1))^2}{4(p \cdot k_1)^2} \right] \Theta_\Delta(k_1). \quad (85)$$

Adding Eqs. (67) and (85), we find that $[(\delta m^2)_{3a} + (\delta m^2)_{3b}]^I + [(\delta m^2)'_{8a} + (\delta m^2)'_{8b}]^I$ is IR finite.

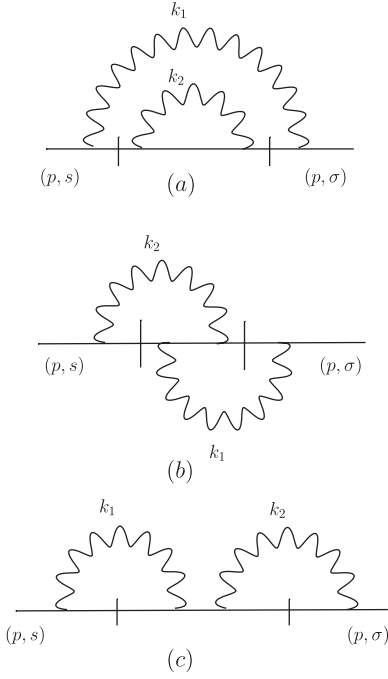


FIG. 7. Diagrams for $O(e^4)$ self-energy correction in the Fock basis corresponding to T_7 .

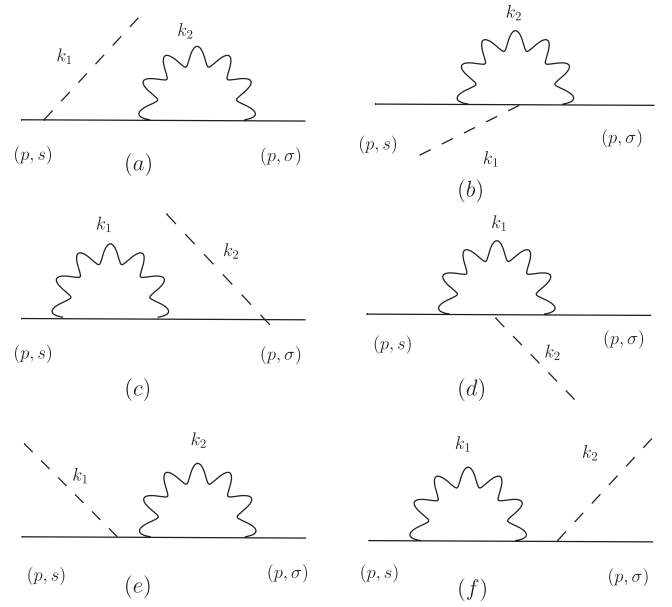


FIG. 8. Additional diagrams in the coherent state basis for $O(e^4)$ self-energy correction corresponding to T_8 .

Adding all the contributions coming from Figs. 3, 8, and 9, we find that the IR divergences completely cancel. Below, we summarize this result for the reader's convenience:

- (1) $[(\delta m^2)_{3a} + (\delta m^2)_{3b}]^I + [(\delta m^2)'_{8a} + (\delta m^2)'_{8b}]^I$ is IR finite.
- (2) $[(\delta m^2)_{3a} + (\delta m^2)_{3b}]^{II} + [(\delta m^2)'_{8c} + (\delta m^2)'_{8d}]^{II}$ is IR finite.
- (3) $[(\delta m^2)_{3c}]^I + [(\delta m^2)'_{8e}]^I$ is IR finite.
- (4) $[(\delta m^2)_{3c}]^{II} + [(\delta m^2)'_{8f}]^{II}$ is IR finite.
- (5) $[(\delta m^2)_3]^{III} + [(\delta m^2)'_{8a} + (\delta m^2)'_{8b}]^{III} + [(\delta m^2)'_{8e}]^{III}$ is IR finite.
- (6) $[(\delta m^2)'_{8c} + (\delta m^2)'_{8d}]^{III} + [(\delta m^2)'_{8f}]^{III} + [(\delta m^2)'_9]^{III}$ is IR finite.

Thus, we can see that the self-energy correction corresponding to three-point QED vertices up to $O(e^4)$ is IR finite. In the same manner, we can show the cancellation of IR divergences for diagrams containing a four-point instantaneous fermion exchange vertex in all the three limits. We give here one calculation for illustration. The contributions corresponding to Fig. 10 are given by

$$(\delta m^2)'_{10} = (\delta m^2)'_{10a} + (\delta m^2)'_{10b} + (\delta m^2)'_{10c} + (\delta m^2)'_{10d} + (\delta m^2)'_{10e} + (\delta m^2)'_{10f} + (\delta m^2)'_{10g} \\ + (\delta m^2)'_{10h} + (\delta m^2)'_{10i} + (\delta m^2)'_{10j}. \quad (86)$$

As shown in Appendix D, the IR divergent contributions in Figs. 10(a), 10(c), 10(e), and 10(g) in the limit I are given by the following expressions:

$$[(\delta m^2)'_{10a}]^I = [(\delta m^2)'_{10g}]^I \\ = \frac{e^4}{(2\pi)^6} \int d^2\mathbf{k}_{1\perp} d^2\mathbf{k}_{2\perp} \int \frac{dk_1^+}{k_1^+} \frac{dk_2^+}{k_2^+} \frac{[2p^+(p \cdot \epsilon(k_1))(p \cdot \epsilon(k_2))(\epsilon(k_1) \cdot \epsilon(k_2)) + k_2^+(p \cdot \epsilon(k_1))^2]}{8p^+(p \cdot k_1)(p \cdot k_2)} \Theta_{\Delta}(k_1), \quad (87)$$

$$[(\delta m^2)'_{10c}]^I = \frac{e^4}{(2\pi)^6} \int d^2\mathbf{k}_{1\perp} d^2\mathbf{k}_{2\perp} \int \frac{dk_1^+}{k_1^+} \frac{dk_2^+}{k_2^+} \frac{[2p^+(p \cdot \epsilon(k_1))(p \cdot \epsilon(k_2))(\epsilon(k_1) \cdot \epsilon(k_2)) + k_2^+(p \cdot \epsilon(k_1))^2]}{8p^+(p \cdot k_1)(p \cdot k_2)} \Theta_{\Delta}(k_1), \quad (88)$$

$$[(\delta m^2)'_{10e}]^I = \frac{e^4}{(2\pi)^6} \int d^2\mathbf{k}_{1\perp} d^2\mathbf{k}_{2\perp} \int \frac{dk_1^+}{k_1^+} \frac{dk_2^+}{k_2^+} \frac{[2p_3^+(p \cdot \epsilon(k_1))(p \cdot \epsilon(k_2))(\epsilon(k_1) \cdot \epsilon(k_2)) - k_2^+(p \cdot \epsilon(k_1))^2]}{8p_3^+(p \cdot k_1)(p \cdot k_2)} \Theta_\Delta(k_1). \quad (89)$$

Adding Eqs. (73)–(75) and (87)–(89), we find that $[(\delta m^2)_{4a}]^I + [(\delta m^2)_{5a}]^I + [(\delta m^2)_{5b}]^I + [(\delta^2)_{6a}]^I + [(\delta m^2)'_{10a}]^I + [(\delta m^2)'_{10e}]^I + [(\delta m^2)'_{10g}]^I + [(\delta m^2)'_{10c}]^I + [(\delta m^2)'_{10e}]^I + [(\delta m^2)'_{10g}]^I$ is IR finite. Adding all the contributions from Figs. 4–6, 10, and 11, we find that the IR divergences exactly cancel. Below, we summarize our results:

- (1) $[(\delta m^2)_{4a}]^I + [(\delta m^2)_{5a}]^I + [(\delta m^2)_{5b}]^I + [(\delta^2)_{6a}]^I + [(\delta m^2)'_{10a}]^I + [(\delta m^2)'_{10c}]^I + [(\delta m^2)'_{10e}]^I + [(\delta m^2)'_{10g}]^I$ is IR finite.
- (2) $[(\delta m^2)_{4b}]^{II} + [(\delta m^2)_{5a}]^{II} + [(\delta m^2)_{5b}]^{II} + [(\delta m^2)_{6b}]^{II} + [(\delta m^2)'_{10b}]^{II} + [(\delta m^2)'_{10d}]^{II} + [(\delta m^2)'_{10f}]^{II} + [(\delta m^2)'_{10h}]^{II}$ is IR finite.
- (3) $[(\delta m^2)_{4c}]^I + [(\delta m^2)_{5c}]^I + [(\delta m^2)_{6c}]^I + [(\delta m^2)'_{10i}]^I + [(\delta m^2)'_{10j}]^I$ is IR finite.
- (4) $[(\delta m^2)_4 + (\delta m^2)_5 + (\delta m^2)_6 + (\delta m^2)'_{10} + (\delta m^2)'_{11}]^{III}$ is IR finite.

Thus, finally we obtain that

$$(\delta m^2)^{(2)} + \sum_{i=8}^{11} (\delta m^2)'_i,$$

is IR finite, where $(\delta m^2)^{(2)}$ is the $O(e^4)$ electron mass correction in the Fock basis. This completes the proof of cancellation of true IR divergences up to $O(e^4)$ for fermion self-energy correction in the coherent state basis.

VII. CONCLUSION

We have calculated the electron self-energy correction in light-front QED up to $O(e^4)$ and have shown that the true IR divergences get canceled when the coherent state basis is used to calculate the matrix elements. The cancellation of IR divergences between real and virtual processes is known to hold in equal-time QED to all orders. This cancellation was also shown by KF [3] using the coherent state formalism. It would be interesting to verify this all-order cancellation in LFQED. The present work is a first step towards this aim. The true IR divergences in QCD do not cancel in higher orders. This fact can possibly be used to obtain a form of the artificial potential required for the bound state calculation. The connection between the asymptotic dynamics and cancellation/noncancellation of

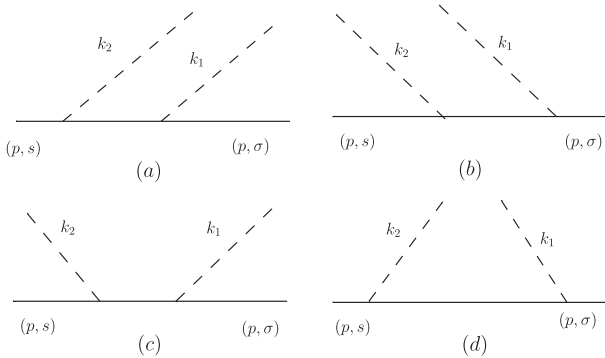


FIG. 9. Additional diagrams in the coherent state basis for $O(e^4)$ self-energy correction corresponding to T_9 .

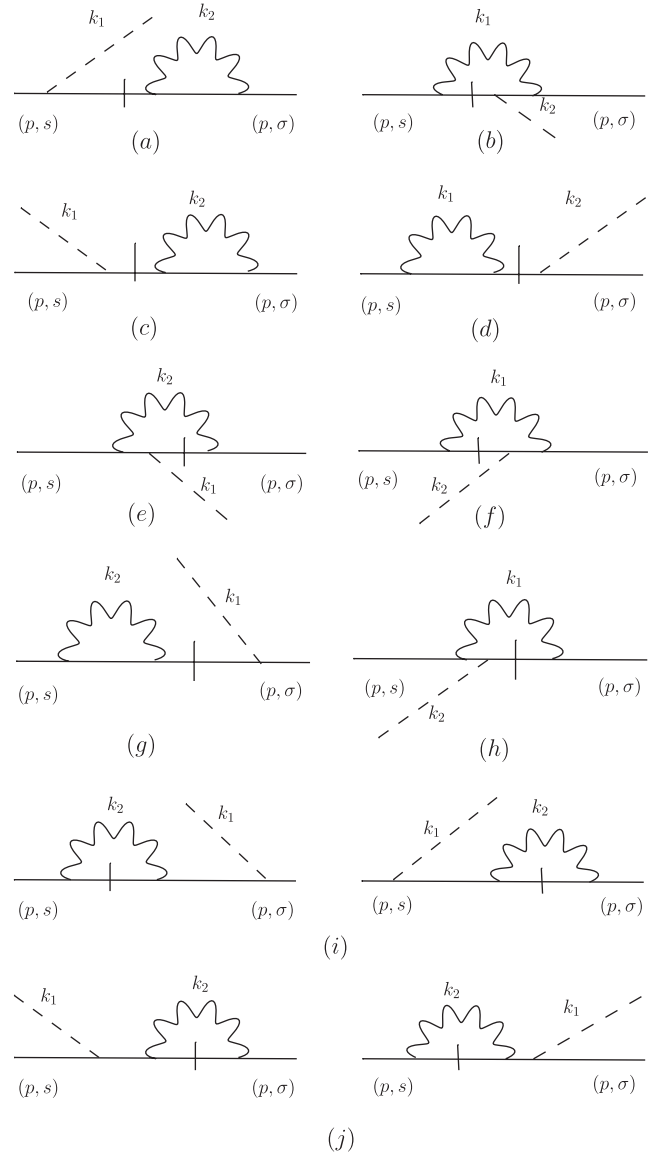


FIG. 10. Additional diagrams in the coherent state basis for $O(e^4)$ self-energy correction corresponding to T_{10} .

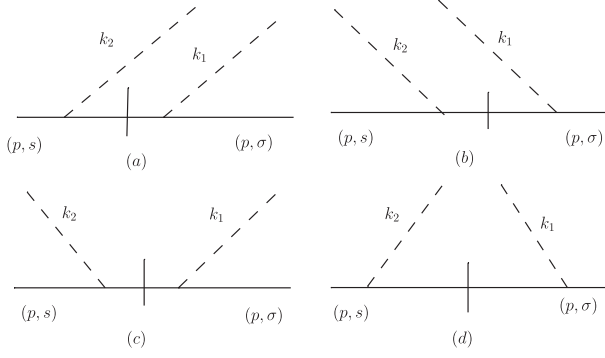


FIG. 11. Additional diagrams in the coherent state basis for $O(e^4)$ self-energy correction corresponding to T_{11} .

IR divergences can also be exploited to explore the possibility of constructing an artificial potential which is used in the bound state calculations in LFQCD [26].

ACKNOWLEDGMENTS

We wish to acknowledge the financial support from the Department of Science and Technology, India, under Grant No. SR/S2/HEP-17/2006.

APPENDIX A: NOTATION AND USEFUL RELATIONS

We define the four-vector x^μ by

$$x^\mu = (x^0, x^3, x^1, x^2) = (x^0, x^3, \mathbf{x}^\perp).$$

The light-front variables are defined by

$$x^+ = \frac{(x^0 + x^3)}{\sqrt{2}}, \quad x^- = \frac{(x^0 - x^3)}{\sqrt{2}}, \quad \mathbf{x}_\perp = (x^1, x^2). \quad (\text{A1})$$

Thus, in light-front variables,

$$x^\mu = (x^+, x^-, \mathbf{x}^\perp).$$

The metric tensor is

$$g^{\mu\nu} = \begin{bmatrix} 0 & 1 & 0 & 0 \\ 1 & 0 & 0 & 0 \\ 0 & 0 & -1 & 0 \\ 0 & 0 & 0 & -1 \end{bmatrix}.$$

A. Dirac spinors

$u(p, s)$ and $\bar{u}(p, s)$ satisfy the usual properties

$$(\not{p} - m)u(p, s) = 0, \quad (\not{p} + m)v(p, s) = 0, \quad (\text{A2})$$

$$\begin{aligned} \bar{u}(p, s)u(p, s') &= -\bar{v}(p, s)v(p, s') = 2m\delta_{ss'}, \\ \bar{u}(p, s)\gamma^\mu u(p, s') &= \bar{v}(p, s)\gamma^\mu v(p, s') = 2p^\mu\delta_{ss'}, \end{aligned} \quad (\text{A3})$$

$$\begin{aligned} \sum_{s=\pm 1/2} u(p, s)\bar{u}(p, s) &= \not{p} + m, \\ \sum_{s=\pm 1/2} v(p, s)\bar{v}(p, s) &= \not{p} - m. \end{aligned} \quad (\text{A4})$$

B. Photon polarizations

The photon polarization tensor ϵ_μ^λ satisfies

$$d_{\mu\nu}(p) = \sum_{\lambda=1,2} \epsilon_\mu^\lambda(p)\epsilon_\nu^\lambda(p) = -g_{\mu\nu} + \frac{\delta_{\mu+}p_\nu + \delta_{\nu+}p_\mu}{p^+}. \quad (\text{A5})$$

Some useful properties satisfied by $d_{\alpha\beta}(p)$ are

$$\gamma^\alpha \gamma^\beta d_{\alpha\beta}(p) = -2, \quad (\text{A6})$$

$$\gamma^\alpha \gamma^\nu \gamma^\beta d_{\alpha\beta}(p) = \frac{2}{p^+}(\gamma^+ p^\nu + g^{+\nu} \not{p}), \quad (\text{A7})$$

$$\begin{aligned} \gamma^\alpha \gamma^\mu \gamma^\nu \gamma^\beta d_{\alpha\beta}(p) &= -4g^{\mu\nu} + \frac{2p_\alpha}{p^+}(g^{\mu\alpha}\gamma^\nu\gamma^+ \\ &\quad - g^{\alpha\nu}\gamma^\mu\gamma^+ + g^{\alpha+}\gamma^\mu\gamma^\nu \\ &\quad - g^{+\nu}\gamma^\mu\gamma^\alpha + g^{+\mu}\gamma^\nu\gamma^\alpha). \end{aligned} \quad (\text{A8})$$

C. Energy denominators

We will need the following expressions for energy denominators:

$$p^- - k_1^- - (p - k_1)^- = -\frac{(p \cdot k_1)}{p^+ - k_1^+}, \quad (\text{A9})$$

$$\begin{aligned} p^- - k_1^- - k_2^- - (p - k_1 - k_2)^- \\ &= -\frac{p \cdot k_1 + p \cdot k_2 - k_1 \cdot k_2}{p^+ - k_1^+ - k_2^+}, \\ p^- + k_1^- - k_2^- - (p + k_1 - k_2)^- \\ &= \frac{p \cdot k_1 - p \cdot k_2 - k_1 \cdot k_2}{p^+ + k_1^+ - k_2^+}, \\ p^- - k_1^- + k_2^- - (p - k_1 + k_2)^- \\ &= -\frac{p \cdot k_1 - p \cdot k_2 + k_1 \cdot k_2}{p^+ - k_1^+ + k_2^+}, \\ p^- + k_1^- + k_2^- - (p + k_1 + k_2)^- \\ &= \frac{p \cdot k_1 + p \cdot k_2 + k_1 \cdot k_2}{p^+ + k_1^+ + k_2^+}. \end{aligned} \quad (\text{A10})$$

APPENDIX B: PROPERTIES OF COHERENT STATES

The coherent state containing a fermion and the superposition of an infinite number of soft photons is denoted by

$|1: p_i\rangle$ and is defined by Eq. (52). Similarly, the coherent state containing a fermion and a hard photon is denoted by $|2: p_i, k_i\rangle$. The coherent states $|1: p_i\rangle$ are the eigenstates of $a(k, \lambda)$ [11]:

$$a(k, \rho)|1: p_i\rangle = -\frac{e}{(2\pi)^{3/2}} \frac{f(k, \rho: p_i)}{\sqrt{2k^+}} |1: p_i\rangle. \quad (\text{B1})$$

Also,

$$a(k, \rho)|2: p_i, k_i\rangle = -\frac{e}{(2\pi)^{3/2}} \frac{f(k, \rho: p_i)}{\sqrt{2k^+}} |2: p_i, k_i\rangle + \delta^3(k - k_i) \delta_{\rho\lambda_i} |1: p_i\rangle, \quad (\text{B2})$$

and

$$a^\dagger(k, \rho)|1: p_i\rangle = \frac{e}{(2\pi)^{3/2}} \frac{f^*(k, \rho: p_i)}{\sqrt{2k^+}} |1: p_i\rangle + |2: p_i, k_i\rangle, \quad (\text{B3})$$

$$a^\dagger(k, \rho)|2: p_i, k_i\rangle = \frac{e}{(2\pi)^{3/2}} \frac{f^*(k, \rho: p_i)}{\sqrt{2k^+}} |2: p_i, k_i\rangle + |3: p_i, k_i, k_j\rangle. \quad (\text{B4})$$

Coherent states satisfy the following orthonormalization properties:

$$\langle 1: p_f, \sigma_f | 1: p_i, \sigma_i \rangle = \delta^{(3)}(p_i - p_f) \delta_{\sigma_i \sigma_f}, \quad (\text{B5})$$

$$\begin{aligned} \langle 1: p_f, \sigma_f | 2: p_i, \sigma_i, k_i, \lambda_i \rangle \\ = \frac{e}{(2\pi)^{3/2}} \frac{f(k_i, \lambda_i: p_i)}{\sqrt{2k_i^+}} \delta^{(3)}(p_i - p_f) \delta_{\sigma_i \sigma_f}. \end{aligned} \quad (\text{B6})$$

APPENDIX C: TRANSITION MATRIX ELEMENT IN THE FOCK BASIS FOR SELF-ENERGY UP TO $\mathcal{O}(e^4)$

We now calculate T_3 , which is defined by Eq. (58) and corresponds to Fig. 3. Inserting complete sets of intermediate states in T_3 , we obtain

$$T_3(p, p) = T_{3a} + T_{3b} + T_{3c},$$

where

$$\begin{aligned} T_{3a} = \frac{e^4}{(2\pi)^6} \int \frac{d^2\mathbf{k}_{1\perp} d^2\mathbf{k}_{2\perp}}{2p^+} \int \frac{dk_1^+ dk_2^+}{32k_1^+ k_2^+ p_1^+ p_2^+ p_3^+} \\ \times \frac{\bar{u}(p, s) [\not{\epsilon}^{\lambda_1}(k_1)(\not{p}_1 + m) \not{\epsilon}^{\lambda_2}(k_2)(\not{p}_2 + m) \not{\epsilon}^{\lambda_2}(k_2)(\not{p}_1 + m) \not{\epsilon}^{\lambda_1}(k_1)] u(p, s)}{(p^- - p_1^- - k_1^-)(p^- - p_2^- - k_1^- - k_2^-)(p^- - p_1^- - k_1^-)}, \end{aligned} \quad (\text{C1})$$

with

$$p_1 = p - k_1, \quad (\text{C2})$$

$$p_2 = p - k_1 - k_2. \quad (\text{C3})$$

Similarly,

$$\begin{aligned} T_{3b} = \frac{e^4}{(2\pi)^6} \int \frac{d^2\mathbf{k}_{1\perp} d^2\mathbf{k}_{2\perp}}{2p^+} \int \frac{dk_1^+ dk_2^+}{32k_1^+ k_2^+ p_1^+ p_2^+ p_3^+} \\ \times \frac{\bar{u}(p, s) [\not{\epsilon}^{\lambda_2}(k_2)(\not{p}_3 + m) \not{\epsilon}^{\lambda_1}(k_1)(\not{p}_2 + m) \not{\epsilon}^{\lambda_2}(k_2)(\not{p}_1 + m) \not{\epsilon}^{\lambda_1}(k_1)] u(p, s)}{(p^- - p_1^- - k_1^-)(p^- - p_3^- - k_2^-)(p^- - p_2^- - k_1^- - k_2^-)}, \end{aligned} \quad (\text{C4})$$

with

$$p_3 = p - k_2, \quad (\text{C5})$$

$$\begin{aligned} T_{3c} = \frac{e^4}{(2\pi)^6} \int \frac{d^2\mathbf{k}_{1\perp} d^2\mathbf{k}_{2\perp}}{2p^+} \int \frac{dk_1^+ dk_2^+}{32k_1^+ k_2^+ p_1^+ p_3^+ p^+} \\ \times \frac{\bar{u}(p, s) [\not{\epsilon}^{\lambda_2}(k_2)(\not{p}_3 + m) \not{\epsilon}^{\lambda_2}(k_2)(\not{p}' + m) \not{\epsilon}^{\lambda_1}(k_1)(\not{p}_1 + m) \not{\epsilon}^{\lambda_1}(k_1)] u(p, s)}{(p^- - p_1^- - k_1^-)(p^- - p_2'^-)(p^- - p_3^- - k_2^-)}. \end{aligned} \quad (\text{C6})$$

In limit I, Eqs. (C1) and (C4) can be added such that the denominator reduces to $(p \cdot k_1)^2 (p \cdot k_2)$. Using Eqs. (A4), (A9), (A10), and (18), we obtain

$$[(\delta m^2)_{3a} + (\delta m^2)_{3b}]^I = -\frac{e^4}{2(2\pi)^6} \int d^2\mathbf{k}_{1\perp} d^2\mathbf{k}_{2\perp} \int \frac{dk_1^+ dk_2^+}{32k_1^+ k_2^+} \times \frac{\text{Tr}[\not{\epsilon}^{\lambda_1}(k_1)(\not{p} + m)\not{\epsilon}^{\lambda_2}(k_2)(\not{p}_3 + m)\not{\epsilon}^{\lambda_2}(k_2)(\not{p} + m)\not{\epsilon}^{\lambda_1}(k_1)(\not{p} + m)]}{(p \cdot k_1)^2(p \cdot k_2)}. \quad (\text{C7})$$

After calculating the trace, Eq. (C7) leads to

$$[(\delta m^2)_{3a} + (\delta m^2)_{3b}]^I = -\frac{e^4}{(2\pi)^6} \int d^2\mathbf{k}_{1\perp} d^2\mathbf{k}_{2\perp} \int \frac{dk_1^+}{k_1^+} \frac{dk_2^+}{k_2^+} \frac{[2(p \cdot \epsilon(k_1))^2(p \cdot \epsilon(k_2))^2 - (p \cdot k_2)(p \cdot \epsilon(k_1))^2]}{4(p \cdot k_1)^2(p \cdot k_2)}. \quad (\text{C8})$$

Again, in limit II, the denominator in the sum of Eqs. (C1) and (C4) reduces to $(p \cdot k_1)(p \cdot k_2)^2$, leading to

$$[(\delta m^2)_{3a} + (\delta m^2)_{3b}]^{II} = -\frac{e^4}{2(2\pi)^6} \int d^2\mathbf{k}_{1\perp} d^2\mathbf{k}_{2\perp} \int \frac{dk_1^+ dk_2^+}{32k_1^+ k_2^+} \times \frac{\text{Tr}[\not{\epsilon}^{\lambda_2}(k_2)(\not{p} + m)\not{\epsilon}^{\lambda_1}(k_1)(\not{p}_1 + m)\not{\epsilon}^{\lambda_2}(k_2)(\not{p}_1 + m)\not{\epsilon}^{\lambda_1}(k_1)(\not{p} + m)]}{(p \cdot k_1)(p \cdot k_2)^2}. \quad (\text{C9})$$

Calculating the trace, Eq. (C9) reduces to

$$[(\delta m^2)_{3a} + (\delta m^2)_{3b}]^{II} = -\frac{e^4}{(2\pi)^6} \int d^2\mathbf{k}_{1\perp} d^2\mathbf{k}_{2\perp} \int \frac{dk_1^+}{k_1^+} \frac{dk_2^+}{k_2^+} \frac{[2(p \cdot \epsilon(k_1))^2(p \cdot \epsilon(k_2))^2 - (p \cdot k_1)(p \cdot \epsilon(k_2))^2]}{4(p \cdot k_1)(p \cdot k_2)^2}. \quad (\text{C10})$$

In limit III, we obtain

$$[(\delta m^2)_{3a} + (\delta m^2)_{3b}]^{III} = -\frac{e^4}{(2\pi)^6} \int d^2\mathbf{k}_{1\perp} d^2\mathbf{k}_{2\perp} \int \frac{dk_1^+}{k_1^+} \frac{dk_2^+}{k_2^+} \frac{(p \cdot \epsilon(k_1))^2(p \cdot \epsilon(k_2))^2}{2(p \cdot k_1)^2(p \cdot k_2)}. \quad (\text{C11})$$

Similarly, T_{3c} leads to

$$\delta m_{3c}^2 = \frac{e^4}{2(2\pi)^6} \int d^2\mathbf{k}_{1\perp} d^2\mathbf{k}_{2\perp} \int \frac{dk_1^+ dk_2^+}{32k_1^+ k_2^+ p_1^+ p_3^+ p^+} \times \frac{\text{Tr}[\not{\epsilon}^{\lambda_2}(k_2)(\not{p}_3 + m)\not{\epsilon}^{\lambda_2}(k_2)(\not{p}' + m)\not{\epsilon}^{\lambda_1}(k_1)(\not{p}_1 + m)\not{\epsilon}^{\lambda_1}(k_1)(\not{p} + m)]}{(p^- - p_1^- - k_1^-)(p^- - p_2^-)(p^- - p_3^- - k_2^-)}, \quad (\text{C12})$$

where p_1 and p_3 are defined by Eqs. (C2) and (C5) and $p_2' = p$. Note that this diagram is one-particle reducible, and therefore the energy denominator associated with the single-particle state vanishes. We shall use the Heitler method [29] for evaluating all such integrals. Using this method, we write [28,29]

$$D = \frac{1}{(p^- - p_2'^-)(p^- - p_1^- - k_1^-)(p^- - p_3^- - k_2^-)} = \int dp'^- \delta(p'^- - p^-) \frac{\mathcal{P}}{(p'^- - p_2'^-)(p'^- - p_1^- - k_1^-)(p'^- - p_3^- - k_2^-)}. \quad (\text{C13})$$

Using the relation between distributions,

$$\frac{\mathcal{P}}{(p'^- - p_2'^-)} \delta(p'^- - p^-) = -\frac{1}{2} \delta'(p'^- - p^-), \quad (\text{C14})$$

and integrating by parts, we obtain

$$D = \frac{1}{2} \int dp'^- \delta(p'^- - p^-) \frac{d}{dp'^-} \left[\frac{1}{(p'^- - p_1^- - k_1^-)(p'^- - p_3^- - k_2^-)} \right] = -\frac{1}{2(p^- - p_1^- - k_1^-)^2(p^- - p_3^- - k_2^-)} - \frac{1}{2(p^- - p_1^- - k_1^-)(p^- - p_3^- - k_2^-)^2}. \quad (\text{C15})$$

Using Eq. (A9) in Eq. (C12), we obtain

$$D = \frac{p_1^+}{2(p \cdot k_1)^2(p \cdot k_2)} + \frac{p_3^+}{2(p \cdot k_1)(p \cdot k_2)^2}. \quad (\text{C16})$$

Thus, in limit I, Eq. (C12) becomes

$$[(\delta m^2)_{3c}]^I = \frac{e^4}{(2\pi)^6} \int d^2\mathbf{k}_{1\perp} d^2\mathbf{k}_{2\perp} \int \frac{dk_1^+}{k_1^+} \frac{dk_2^+}{k_2^+} \frac{2(p \cdot \epsilon(k_1))^2(p \cdot \epsilon(k_2))^2 - (p \cdot k_2)(p \cdot \epsilon(k_1))^2}{8p^+} \\ \times \left[\frac{p^+}{(p \cdot k_1)^2(p \cdot k_2)} + \frac{p_3^+}{(p \cdot k_1)(p \cdot k_2)^2} \right]. \quad (\text{C17})$$

Similarly, in limit II, Eq. (C12) leads to

$$[(\delta m^2)_{3c}]^{II} = \frac{e^4}{(2\pi)^6} \int d^2\mathbf{k}_{1\perp} d^2\mathbf{k}_{2\perp} \int \frac{dk_1^+}{k_1^+} \frac{dk_2^+}{k_2^+} \frac{2(p \cdot \epsilon(k_1))^2(p \cdot \epsilon(k_2))^2 - (p \cdot k_1)(p \cdot \epsilon(k_2))^2}{8p^+} \\ \times \left[\frac{p_1^+}{(p \cdot k_1)^2(p \cdot k_2)} + \frac{p^+}{(p \cdot k_1)(p \cdot k_2)^2} \right], \quad (\text{C18})$$

and in limit III, it gives

$$[(\delta m^2)_{3c}]^{III} = \frac{e^4}{(2\pi)^6} \int d^2\mathbf{k}_{1\perp} d^2\mathbf{k}_{2\perp} \int \frac{dk_1^+}{k_1^+} \frac{dk_2^+}{k_2^+} \left[\frac{(p \cdot \epsilon(k_1))^2(p \cdot \epsilon(k_2))^2}{4(p \cdot k_1)^2(p \cdot k_2)} + \frac{(p \cdot \epsilon(k_1))^2(p \cdot \epsilon(k_2))^2}{4(p \cdot k_1)(p \cdot k_2)^2} \right]. \quad (\text{C19})$$

The traces are calculated using MATHEMATICA.

The contribution to the corresponding diagrams in Fig. 4 is given by

$$(\delta m^2)_4 = (\delta m^2)_{4a} + (\delta m^2)_{4b} + (\delta m^2)_{4c}.$$

In limit I, $(\delta m^2)_{4a}$ reduces to

$$[(\delta m^2)_{4a}]^I = -\frac{e^4}{(2\pi)^6} \int d^2\mathbf{k}_{1\perp} d^2\mathbf{k}_{2\perp} \int \frac{dk_1^+}{k_1^+} \frac{dk_2^+}{k_2^+} \frac{[2p^+(p \cdot \epsilon(k_1))(p \cdot \epsilon(k_2))(\epsilon(k_1) \cdot \epsilon(k_2)) + k_2^+(p \cdot \epsilon(k_1))^2]}{8p^+(p \cdot k_1)(p \cdot k_2)}. \quad (\text{C20})$$

Note that $(\delta m^2)_{4a}$ is not IR divergent when $p \cdot k_1 \neq 0$, even if $p \cdot k_2 = 0$. In limit II, $(\delta m^2)_{4b}$ reduces to

$$[(\delta m^2)_{4b}]^{II} = \frac{e^4}{(2\pi)^6} \int d^2\mathbf{k}_{1\perp} d^2\mathbf{k}_{2\perp} \int \frac{dk_1^+}{k_1^+} \frac{dk_2^+}{k_2^+} \frac{[2p_1^+(p \cdot \epsilon(k_1))(p \cdot \epsilon(k_2))(\epsilon(k_1) \cdot \epsilon(k_2)) - k_1^+(p \cdot \epsilon(k_2))^2]}{8p_1^+(p \cdot k_1)(p \cdot k_2)}. \quad (\text{C21})$$

Note that $(\delta m^2)_{4b}$ is not IR divergent when $p \cdot k_2 \neq 0$, even if $p \cdot k_1 = 0$. In limit III, and after adding the contributions from Figs. 4(a) and 4(b), we get

$$[(\delta m^2)_{4a} + (\delta m^2)_{4b}]^{III} = -\frac{e^4}{(2\pi)^6} \int d^2\mathbf{k}_{1\perp} d^2\mathbf{k}_{2\perp} \int \frac{dk_1^+}{k_1^+} \frac{dk_2^+}{k_2^+} \frac{[(p \cdot \epsilon(k_1))(p \cdot \epsilon(k_2))(\epsilon(k_1) \cdot \epsilon(k_2))]}{4(p \cdot k_1)(p \cdot k_2)}. \quad (\text{C22})$$

For $(\delta m^2)_{4c}$, we use the Heitler method illustrated in Eqs. (C13)–(C15) and obtain

$$(\delta m^2)_{4c} = \frac{e^4}{2(2\pi)^6} \int d^2\mathbf{k}_{1\perp} d^2\mathbf{k}_{2\perp} \int \frac{dk_1^+ dk_2^+}{32k_1^+ k_2^+ p^+} \frac{\text{Tr}[\not{\epsilon}^{\lambda_1}(k_1)(\not{p} + m)\not{\epsilon}^{\lambda_1}(k_1)(\not{p} + m)\not{\epsilon}^{\lambda_2}(k_2)\gamma^+\not{\epsilon}^{\lambda_2}(k_2)(\not{\epsilon} + m)]}{(p \cdot k_1)^2}, \quad (\text{C23})$$

which finally leads to

$$[(\delta m^2)_{4c}]^I = -\frac{e^4}{(2\pi)^6} \int d^2\mathbf{k}_{1\perp} d^2\mathbf{k}_{2\perp} \int \frac{dk_1^+}{k_1^+} \frac{dk_2^+}{k_2^+} \frac{(p \cdot \epsilon(k_1))^2}{8(p \cdot k_1)^2}. \quad (\text{C24})$$

Similarly, the contribution from Figs. 5(a)–5(c) is given by

$$(\delta m^2)_5 = (\delta m^2)_{5a} + (\delta m^2)_{5b} + (\delta m^2)_{5c}.$$

In limit I, $(\delta m^2)_{5a}$ reduces to

$$[(\delta m^2)_{5a}]^I = -\frac{e^4}{(2\pi)^6} \int d^2\mathbf{k}_{1\perp} d^2\mathbf{k}_{2\perp} \int \frac{dk_1^+}{k_1^+} \frac{dk_2^+}{k_2^+} \frac{[2p^+(p \cdot \epsilon(k_1))(p \cdot \epsilon(k_2))(\epsilon(k_1) \cdot \epsilon(k_2)) + k_2^+(p \cdot \epsilon(k_1))^2]}{8p^+(p \cdot k_1)(p \cdot k_2)}. \quad (\text{C25})$$

Similarly, in limit II we get

$$[(\delta m^2)_{5a}]^{II} = -\frac{e^4}{(2\pi)^6} \int d^2\mathbf{k}_{1\perp} d^2\mathbf{k}_{2\perp} \int \frac{dk_1^+}{k_1^+} \frac{dk_2^+}{k_2^+} \frac{[2p^+(p \cdot \epsilon(k_1))(p \cdot \epsilon(k_2))(\epsilon(k_1) \cdot \epsilon(k_2)) + k_1^+(p \cdot \epsilon(k_2))^2]}{8p_1^+(p \cdot k_1)(p \cdot k_2)}, \quad (C26)$$

and in limit III we get

$$[(\delta m^2)_{5a}]^{III} = \frac{e^4}{(2\pi)^6} \int d^2\mathbf{k}_{1\perp} d^2\mathbf{k}_{2\perp} \int \frac{dk_1^+}{k_1^+} \frac{dk_2^+}{k_2^+} \frac{[(p \cdot \epsilon(k_1))(p \cdot \epsilon(k_2))(\epsilon(k_1) \cdot \epsilon(k_2))]}{4(p \cdot k_1)(p \cdot k_2)}. \quad (C27)$$

Taking limit I $(\delta m^2)_{5b}$ reduces to

$$[(\delta m^2)_{5b}]^I = -\frac{e^4}{(2\pi)^6} \int d^2\mathbf{k}_{1\perp} d^2\mathbf{k}_{2\perp} \int \frac{dk_1^+}{k_1^+} \frac{dk_2^+}{k_2^+} \frac{[2p_3^+(p \cdot \epsilon(k_1))(p \cdot \epsilon(k_2))(\epsilon(k_1) \cdot \epsilon(k_2)) - k_2^+(p \cdot \epsilon(k_1))^2]}{8p_3^+(p \cdot k_1)(p \cdot k_2)}. \quad (C28)$$

Taking limit II, we get

$$[(\delta m^2)_{5b}]^{II} = -\frac{e^4}{(2\pi)^6} \int d^2\mathbf{k}_{1\perp} d^2\mathbf{k}_{2\perp} \int \frac{dk_1^+}{k_1^+} \frac{dk_2^+}{k_2^+} \frac{[2p_1^+(p \cdot \epsilon(k_1))(p \cdot \epsilon(k_2))(\epsilon(k_1) \cdot \epsilon(k_2)) - k_1^+(p \cdot \epsilon(k_2))^2]}{8p_1^+(p \cdot k_1)(p \cdot k_2)}, \quad (C29)$$

and taking limit III, we get

$$[(\delta m^2)_{5b}]^{III} = -\frac{e^4}{(2\pi)^6} \int d^2\mathbf{k}_{1\perp} d^2\mathbf{k}_{2\perp} \int \frac{dk_1^+}{k_1^+} \frac{dk_2^+}{k_2^+} \frac{[(p \cdot \epsilon(k_1))(p \cdot \epsilon(k_2))(\epsilon(k_1) \cdot \epsilon(k_2))]}{4(p \cdot k_1)(p \cdot k_2)}. \quad (C30)$$

$(\delta m^2)_{5c}$ in limit I reduces to

$$[(\delta m^2)_{5c}]^I = \frac{e^4}{(2\pi)^6} \int d^2\mathbf{k}_{1\perp} d^2\mathbf{k}_{2\perp} \int \frac{dk_1^+}{k_1^+} \frac{dk_2^+}{k_2^+} \frac{(p \cdot \epsilon(k_1))^2}{4(p \cdot k_1)^2}. \quad (C31)$$

The contribution of Figs. 6(a)–6(c) is given by

$$(\delta m^2)_6 = (\delta m^2)_{6a} + (\delta m^2)_{6b} + (\delta m^2)_{6c}.$$

In limit I, $(\delta m^2)_{6a}$ reduces to

$$[(\delta m^2)_{6a}]^I = -\frac{e^4}{(2\pi)^6} \int d^2\mathbf{k}_{1\perp} d^2\mathbf{k}_{2\perp} \int \frac{dk_1^+}{k_1^+} \frac{dk_2^+}{k_2^+} \frac{[2p^+(p \cdot \epsilon(k_1))(p \cdot \epsilon(k_2))(\epsilon(k_1) \cdot \epsilon(k_2)) + k_2^+(p \cdot \epsilon(k_1))^2]}{8p^+(p \cdot k_1)(p \cdot k_2)}. \quad (C32)$$

Note that $(\delta m^2)_{6a}$ is not IR divergent when $p \cdot k_1 \neq 0$, even if $p \cdot k_2 = 0$. In limit II, $(\delta m^2)_{6b}$ reduces to

$$[(\delta m^2)_{6b}]^{II} = -\frac{e^4}{(2\pi)^6} \int d^2\mathbf{k}_{1\perp} d^2\mathbf{k}_{2\perp} \int \frac{dk_1^+}{k_1^+} \frac{dk_2^+}{k_2^+} \frac{[2p_1^+(p \cdot \epsilon(k_1))(p \cdot \epsilon(k_2))(\epsilon(k_1) \cdot \epsilon(k_2)) - k_1^+(p \cdot \epsilon(k_2))^2]}{8p_1^+(p \cdot k_1)(p \cdot k_2)}. \quad (C33)$$

Note that $(\delta m^2)_{6b}$ is not IR divergent when $p \cdot k_2 \neq 0$, even if $p \cdot k_1 = 0$. In limit III, the sum of $(\delta m^2)_{6a}$ and $(\delta m^2)_{6b}$ reduces to

$$[(\delta m^2)_{6a} + (\delta m^2)_{6b}]^{III} = -\frac{e^4}{(2\pi)^6} \int d^2\mathbf{k}_{1\perp} d^2\mathbf{k}_{2\perp} \int \frac{dk_1^+}{k_1^+} \frac{dk_2^+}{k_2^+} \frac{[(p \cdot \epsilon(k_1))(p \cdot \epsilon(k_2))(\epsilon(k_1) \cdot \epsilon(k_2))]}{4(p \cdot k_1)(p \cdot k_2)}. \quad (C34)$$

For Fig. 6(c), we use the Heitler method [28] to obtain the following result in limit I:

$$[(\delta m^2)_{6c}]^I = -\frac{e^4}{(2\pi)^6} \int d^2\mathbf{k}_{1\perp} d^2\mathbf{k}_{2\perp} \int \frac{dk_1^+}{k_1^+} \frac{dk_2^+}{k_2^+} \frac{(p \cdot \epsilon(k_1))^2}{8(p \cdot k_1)^2}. \quad (C35)$$

APPENDIX D: TRANSITION MATRIX IN THE COHERENT STATE BASIS

We will now present the calculation of $(\delta m^2)^{(2)'}_8$, where the prime denotes the extra contribution arising due to use of the coherent state basis. The contribution corresponding to Fig. 8 can be written as

$$(\delta m^2)'_8 = (\delta m^2)'_{8a} + (\delta m^2)'_{8b} + (\delta m^2)'_{8c} + (\delta m^2)'_{8d} + (\delta m^2)'_{8e} + (\delta m^2)'_{8f},$$

where

$$(\delta m^2)'_{8a} = \frac{e^4}{2(2\pi)^6} \int d^2\mathbf{k}_{1\perp} d^2\mathbf{k}_{2\perp} \int \frac{dk_1^+ dk_2^+}{16k_1^+ k_2^+} \frac{\text{Tr}[\not{\epsilon}^{\lambda_2}(k_2)(\not{p}_3 + m)\not{\epsilon}^{\lambda_1}(k_1)(\not{p}_1 + m)\not{\epsilon}^{\lambda_1}(k_1)(\not{p} + m)](p \cdot \epsilon^{\lambda_1}(k_1))\Theta_{\Delta}(k_1)}{(p \cdot k_1)^2[(p \cdot k_1) + (p \cdot k_2) - (k_1 \cdot k_2)]}, \quad (\text{D1})$$

$$(\delta m^2)'_{8b} = \frac{e^4}{2(2\pi)^6} \int d^2\mathbf{k}_{1\perp} d^2\mathbf{k}_{2\perp} \int \frac{dk_1^+ dk_2^+}{16k_1^+ k_2^+} \frac{\text{Tr}[\not{\epsilon}^{\lambda_2}(k_2)(\not{p}_3 + m)\not{\epsilon}^{\lambda_1}(k_1)(\not{p}_3 + m)\not{\epsilon}^{\lambda_2}(k_2)(\not{p} + m)](p \cdot \epsilon^{\lambda_1}(k_1))\Theta_{\Delta}(k_1)}{(p \cdot k_1)(p \cdot k_2)[(p \cdot k_1) + (p \cdot k_2) - (k_1 \cdot k_2)]}. \quad (\text{D2})$$

Calculating the trace, adding Eqs. (D1) and (D2) and taking limit I, we obtain Eq. (85). Similarly, one can obtain the expressions for Figs. 8(c)–8(f) in the appropriate limits. Figure 9 corresponds to the transition matrix element T'_9 , and its contribution is given by

$$(\delta m^2)'_9 = (\delta m^2)'_{9a} + (\delta m^2)'_{9b} + (\delta m^2)'_{9c} + (\delta m^2)'_{9d},$$

where

$$[(\delta m^2)'_{9a}]^{III} = -\frac{e^4}{(2\pi)^6} \int d^2\mathbf{k}_{1\perp} d^2\mathbf{k}_{2\perp} \int \frac{dk_1^+}{k_1^+} \frac{dk_2^+}{k_2^+} \frac{(p \cdot \epsilon(k_1))^2(p \cdot \epsilon(k_2))^2}{4(p \cdot k_1)^2(p \cdot k_2)} \Theta_{\Delta}(k_1)\Theta_{\Delta}(k_2), \quad (\text{D3})$$

$$[(\delta m^2)'_{9b}]^{III} = -\frac{e^4}{(2\pi)^6} \int d^2\mathbf{k}_{1\perp} d^2\mathbf{k}_{2\perp} \int \frac{dk_1^+}{k_1^+} \frac{dk_2^+}{k_2^+} \frac{(p \cdot \epsilon(k_1))^2(p \cdot \epsilon(k_2))^2}{4(p \cdot k_1)^2(p \cdot k_2)} \Theta_{\Delta}(k_1)\Theta_{\Delta}(k_2), \quad (\text{D4})$$

$$[(\delta m^2)'_{9c} + (\delta m^2)'_{9d}]^{III} = \frac{e^4}{(2\pi)^6} \int d^2\mathbf{k}_{1\perp} d^2\mathbf{k}_{2\perp} \int \frac{dk_1^+}{k_1^+} \frac{dk_2^+}{k_2^+} \times \left[\frac{(p \cdot \epsilon(k_1))^2(p \cdot \epsilon(k_2))^2}{4(p \cdot k_1)^2(p \cdot k_2)} + \frac{(p \cdot \epsilon(k_1))^2(p \cdot \epsilon(k_2))^2}{4(p \cdot k_1)(p \cdot k_2)^2} \right] \Theta_{\Delta}(k_1)\Theta_{\Delta}(k_2). \quad (\text{D5})$$

Here we have used the Heitler method to get the above result.

Similarly, the contribution coming from the diagrams in Figs. 10 and 11 can be easily evaluated by taking the appropriate limits.

-
- | | |
|--|--|
| <p>[1] F. Bloch and A. Nordsieck, <i>Phys. Rev.</i> 52, 54 (1937).
 [2] V. Chung, <i>Phys. Rev.</i> 140, B1110 (1965).
 [3] P. P. Kulish and L. D. Faddeev, <i>Theor. Math. Phys.</i> 4, 745 (1970).
 [4] D. R. Butler and C. A. Nelson, <i>Phys. Rev. D</i> 18, 1196 (1978).
 [5] C. A. Nelson, <i>Nucl. Phys.</i> B181, 141 (1981).
 [6] C. A. Nelson, <i>Nucl. Phys.</i> B186, 187 (1981).
 [7] M. Greco, F. Palumbo, G. Pancheri-Srivastava, and Y. Srivastava, <i>Phys. Lett.</i> 77B, 282 (1978).
 [8] H. D. Dahmeim and F. Steiner, <i>Z. Phys. C</i> 11, 247 (1981).
 [9] A. Harindranath and J. P. Vary, <i>Phys. Rev. D</i> 37, 3010 (1988).
 [10] L. Martinovic and J. P. Vary, <i>Phys. Lett. B</i> 459, 186 (1999).
 [11] Anuradha Misra, <i>Phys. Rev. D</i> 50, 4088 (1994).
 [12] Anuradha Misra, <i>Phys. Rev. D</i> 53, 5874 (1996).
 [13] Anuradha Misra, <i>Phys. Rev. D</i> 62, 125017 (2000).</p> | <p>[14] R. Horan, M. Lavelle, and D. McMullan, <i>Pramana J. Phys.</i> 51, 317 (1998).
 [15] R. Horan, M. Lavelle, and D. McMullan, Report No. PLY-MS-99-9, 1999.
 [16] R. Horan, M. Lavelle, and D. McMullan, <i>arXiv:hep-th/0002206</i>.
 [17] Anuradha Misra, <i>Few-Body Syst.</i> 36, 201 (2005).
 [18] P. P. Srivastava and S. J. Brodsky, <i>Phys. Rev. D</i> 64, 045006 (2001).
 [19] S. J. Brodsky, V. A. Franke, J. R. Hiller, G. McCartor, S. A. Paston, and E. V. Prokhvatilov, <i>Nucl. Phys.</i> B703, 333 (2004); S. S. Chabysheva and J. R. Hiller, <i>Phys. Rev. D</i> 79, 114017 (2009); 82, 034004 (2010).
 [20] S. S. Chabysheva and J. R. Hiller, <i>Phys. Rev. D</i> 84, 034001 (2011).
 [21] Anuradha Misra and Swati Warawdekar, <i>Phys. Rev. D</i> 71, 125011 (2005).
 [22] N. E. Ligterink and B. L. G. Bakker, <i>Phys. Rev. D</i> 52, 5954 (1995).
 [23] N. C. J. Schoonderwoerd and B. L. G. Bakker, <i>Phys. Rev. D</i> 57, 4965 (1998).</p> |
|--|--|

- [24] B. L. G. Bakker, M. A. DeWitt, C.-R. Ji, and Y. Mishchenko, [Phys. Rev. D **72**, 076005 \(2005\)](#).
- [25] R. J. Perry, [arXiv:hep-th/9407056v2](#).
- [26] K. G. Wilson, T. S. Walhout, A. Harindranath, W. M. Zhang, R. J. Perry, and St. D. Glazek, [Phys. Rev. D **49**, 6720 \(1994\)](#).
- [27] S. J. Brodsky, H.-C. Pauli, and S. S. Pinsky, [Phys. Rep. **301**, 299 \(1998\)](#).
- [28] D. Mustaki, S. Pinsky, J. Shigemitsu, and K. G. Wilson, [Phys. Rev. D **43**, 3411 \(1991\)](#).
- [29] W. Heitler, *The Quantum Theory Of Radiation* (Oxford University Press, Oxford, England, 1954).